Available online at www.sciencedirect.com
SCIENCE DIRECT®
Coordination Chemistry Reviews 249 (2005) 633–662
COORDINATION CHEMISTRY REVIEWS
www.elsevier.com/locate/ccr

Review

Complementarity of QTAIM and MO theory in the study of bonding in donor–acceptor complexes

Fernando Cortés-Guzmán[a], Richard F.W. Bader[b,*]

[a] *Departamento de Química Orgánica, Facultad de Química, Unversidad Nacional Autónoma de México, Ciudad Universitaria, México D.F. 04510, México*
[b] *Department of Chemistry, McMaster University, Hamilton, Ont., Canada L8S 4M1*

Received 14 August 2004; accepted 16 August 2004
Available online 22 October 2004

Contents

* Corresponding author. Fax: +1 905 522 2509.
E-mail address: bader@mcmaster.ca (R.F.W. Bader).

0010-8545/$ – see front matter
doi:10.1016/j.ccr.2004.08.022

Abstract

The quantum theory of an atom in a molecule, QTAIM, provides chemists with a choice of how to interpret, understand and predict the observations of experimental chemistry. They may continue with the use of subjective orbital *models* and associated energy and charge partitioning schemes, or they may combine the classification and ordering of electronic states obtained from molecular orbital (MO) *theory* with QTAIM to obtain unique physical answers to chemical questions. MO theory provides a prediction and understanding of the electronic structure of atoms and molecules. The eminently useful models that spring from this theory, the ligand field description of the metal complexes for example, set the stage for the application of quantum mechanics to complete our understanding of the properties predicted by wave functions obtained from theory. The paper demonstrates the complementary nature of MO theory and QTAIM, together with the means of bridging the two approaches in a discussion of the bonding in the carbonyl complexes of Cr, Fe and Ni and the metallocene complexes of Fe, Al^+ and Ge. Particular emphasis is placed on the atomic expectation value of the exchange operator that determines the number of electron pairs exchanged between bonded atoms, obviating the need for the terms 'covalency' and 'resonance'.

One side of the dichotomy in approaches, one based on physics the other eschewing it, is illustrated by a quotation from the abstract of a talk presented by Roald Hoffmann at a symposium of the American Chemical Society on 'Contemporary Aspects of Chemical Bonding', Sept. 2003: "And yet the concept of a chem bond, so essential to chem., and with a venerable history, has a life, generating controversy and incredible interest. Even if we can't reduce it to physics. . . . Push the concept to its limits, accept that a bond will be a bond by some criteria, maybe not by others, respect chem tradition, have fun with the richness of something that cannot be defined clearly, and spare us the hype". The abstract laid the groundwork for the message that a chemical bond lies not only beyond the domain of physics but is incapable of precise physical understanding. Whether physics does or does not offer a definition of a *chemical bond*, it does set out the necessary and sufficient conditions for two atoms to be *chemically bonded* to one another, conditions summarised by Slater in terms of the two theorems that are pivotal to the physics of bonding: ". . . both the virial theorem and Feynman's theorem are exact consequences of wave mechanics. Both interpretations agree in pointing to the existence of the overlap charge density as the essential feature in the attraction between the atoms". The attraction leads to a decrease in the potential energy and to the existence of a potential well which, if of a depth greater than that of the zero point energy, guarantees the system possesses an equilibrium structure wherein no Feynman forces act on the nuclei and wherein the bonding can be characterised by all of the criteria set forth by Hoffmann for the chemical bond; length, energy, force constant etc. So this article makes a modest proposal. Reserve the name and concept of a *bond* for use by those who believe that chemistry lies beyond the scope of physics (in spite of their reliance on molecular orbitals and valence bond structures), and reserve the concept of *bonding* for use by those intent on the pursuit and understanding of chemistry using the tools of quantum mechanics.

Keywords: Atoms; Bonding; Electron density; Electron exchange; Structure

1. Purpose of the paper

This paper contrasts the physical understanding of bonding, and of bonding in metal complexes in particular, obtained from a theory defined in terms of the measurable consequences of bonding on the electron density, the quantum theory of atoms in molecules (QTAIM) [1] with the 'orbital approach', the latter not to be confused with *molecular orbital theory*, a theory complementary with QTAIM. The systems chosen for study are the carbonyl complexes of the transition metals chromium, iron and nickel and the cyclopentadienyl complex formed by iron together with the same complexes of the pre- and post-transition metal atoms aluminium and germanium. The carbonyl complexes of Cr, Fe and Ni provide examples of bonding schemes and energy level diagrams of molecular orbital theory that are associated with octahedral, trigonal bipyramidal and tetrahedral geometries. These systems and the metallocenes are used to illustrate the complementary nature of the quantum theory of atoms in molecules and molecular orbital theory in the understanding of bonding.

2. The physics underlying the QTAIM approach

2.1. Quantum mechanics versus orbitals

When the orbital approach is used in an attempt to answer a chemical question, there can be as many different answers as there are attempts, in line with the philosophy espoused by Hoffmann in his statement "accept that a bond will be a bond by some criteria, maybe not by others". A recent, pertinent example is that there are multiple answers to the question of

Nomenclature

Glossary of symbols

CC	charge concentration in $L(r)$
CP	critical point
BCP	bond critical point
E(A)	energy of atom A
G_b	kinetic energy density at BCP
H_b	energy density at BCP
$L(r)$	$-\nabla^2\rho(r)$
l(A)	percent localization of electrons on A
N(A)	electron population of atom A
Q(A)	quadrupolar polarization of atom A
q(A)	charge of atom A
T(A)	electronic kinetic energy of atoms A
V(A)	electronic potential energy of atom A
V_{ee}	electron–electron potential energy
V_{en}	nuclear–electron potential energy
V_{nn}	nuclear–nuclear potential energy
$\Delta(A) = N(A) - \lambda(A)$	number of electrons on A that are delocalized over other atoms
δ(A, B)	electron delocalization index for atoms A and B
λ(A)	electron localization index for atom A
μ(A)	dipolar polarization of atom A
ρ_b	density at BCP
$\in$	bond ellipticity
$\nabla^2\rho_b$	Laplacian at BCP

the order of the Ga–Ga bond complexed with bulky groups [2–4]. If a question can be couched in the language of physics and this particular one can be—then it will have a unique answer if one uses quantum mechanics, rather than orbitals [5]. We neither anticipate nor accept different answers for expectation values that are predicted by quantum mechanics for the total system. Energy is the expectation value of the Hamiltonian operator and, for a given level of theory, this value is unique. What is required is a quantum mechanics of an atom in a molecule [6–8]. Such a theory would enable one to obtain correspondingly unique answers to chemical questions by translating them into the language of physics.

The underlying structure of quantum mechanics is illustrated in Scheme 1. A system is defined by its forces, the forces determining the Hamiltonian in Schrödinger's equation for a time dependent system or one in a stationary state. The molecular Hamiltonian is expressed in terms of the potential energy operators determined by the Coulombic forces between the electrons and nuclei, each system being identified by its unique nuclear–electron potential. The resulting state vector or wave function is expressed as a linear superposition of base states spanning the Hilbert space. Dirac [9] defines an observable to be a linear Hermitian operator expressible in terms of the dynamical variables with a complete set of eigenfunctions, the base states that are employed in the representation of the state vector, a definition prompting the usage 'Dirac observable' [10]. A change in representation of the state vector from one set of base states that are eigenfunctions of one particular set of commuting Dirac observables, to another, is accomplished using Dirac's transformation theory. There is a Dirac observable associated with every property and it acts on a state vector to yield eigenvalues or expectation values that may or may not be measurable. Each observable obeys an equation of motion and it is these equations that yield the theorems of quantum mechanics, examples being the virial theorem and the Ehrenfest force theorem. Through these theorems, one is able to predict and understand the properties of a system and relate the values of the observables to the forces that define the system, an approach exemplified by Slater's quotation in the Abstract regarding the use of virial theorem and the Feynman force theorem to account for bonding between atoms [11].

Given the mathematical scheme of linear operators and state vectors with its associated probability interpretation in Hilbert space, Schwinger has shown that the whole of quantum mechanics as outlined in Scheme 1, from Schrödinger's equation to the commutation relations, can be deduced from a single dynamical principle [12]. Remarkable as this is, Schwinger's new formulation does much more; it enables the extension of quantum mechanics as outlined in Scheme 1

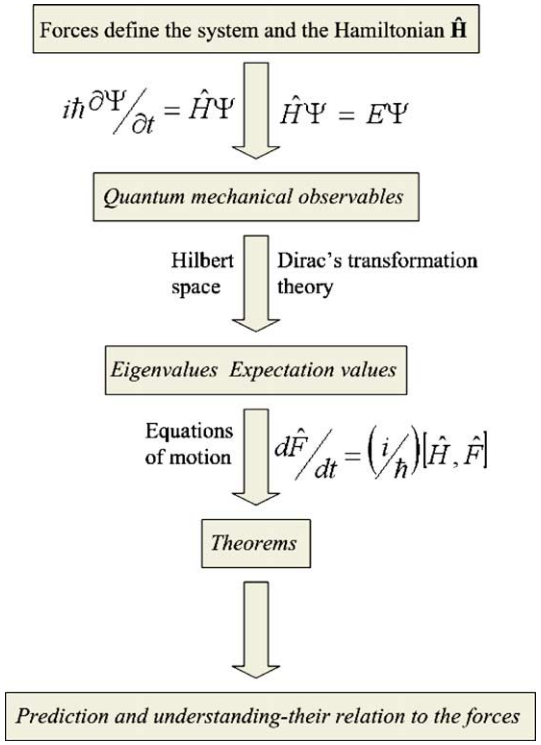

Scheme 1. A schematic representation of the application of quantum mechanics to a particular system, as defined by the forces acting within it. The Scheme applies to both a total system and its component open systems from the line denoted by *eigenvalues and expectation values* downwards, with the boundary of an open system defined by the expectation values of the observable for the electron density.

to an open system. Schrödinger's equation is again obtained for the *total* system in the extension of his principle to an open system. Each Dirac observable, its equation of motion and expectation values are defined for the open system, a bounded piece of the total system [7]. The extension of Schwinger's principle to an open system requires the imposition of a boundary condition and this condition coincides with the topological definition of an atom: a region of space bounded by a surface of local zero flux in the gradient vector field of the density, the zero-flux boundary condition [1,8,13]. It is the extension of Schwinger's principle to an open system that forms the basis for the theory of atoms in molecules by providing the quantum mechanical description of an atom in a molecule. Criticisms of the extension have been responded to in full [14,15]. The properties reported here for the iron atom and carbonyl group in $Fe(CO)_5$ for example, are quantum mechanical expectation values defined on the same footing as are the properties reported for the entire molecule.

2.2. Molecular orbital theory as opposed to orbitals

Orbitals are one-electron states that are used to construct Slater determinants that span the Hilbert space or a truncated portion of it, determinants that are used to approximate the wave function of a many-electron system. Thanks in large to Roothaan [16], molecular orbital (MO) theory is the procedure that is presently used to obtain approximate wave functions, Hartree–Fock or beyond, whose predicted expectation values can be used in the subsequent quantum mechanical analysis outlined in Scheme 1. MO theory provides a prediction, ordering and classification of many-electron states in terms of the component one-electron states, as developed in the early papers of Mulliken [17–19] and Hund [20], work that provides the link with experimental spectroscopy, as admirably illustrated by Herzberg [21]. Changes in the occupations of the Hartree–Fock canonical orbitals may be directly associated with the generation of particular ionised or excited states and provide the energy ordering of transition densities for use in symmetry rules based on second-order perturbation theory [22]. The eminently useful predictive models that come from MO theory, the crystal field/ligand field descriptions of electronic structures of metal complexes and Hückel's $4n + 2$ rule of aromaticity, for example, exemplify the proper use of MO theory—the prediction of a molecule's electronic structure by the successive occupation of the orbitals.

Schrödinger advised against the use of the wave function – a mathematical function in configuration space – however expressed, in any interpretative manner, recommending instead the use of the electron and current densities for this purpose [23]. His advice is not heeded in the 'orbital' approach typical of much of the present literature. This approach is illustrated in a review by Frenking and Frölich [24] that describes the use of orbitals in ways other than those prescribed within *molecular orbital theory*, in the interpretation of bonding in transition-metal molecules and more recently in a paper by Frenking et al. on the analysis of the bonding in donor–acceptor complexes [25]. These papers and others cited therein, will serve as an outline of the traditional approaches to metallic bonding. The 'orbital' approach has recently, been forcefully stated by Frenking [26] in a review of a book by Gillespie and Popelier [27], a book that employs the density and QTAIM in discussing chemical bonding and molecular geometry. Frenking is adamant in his criticism of any approach that uses the electron density because it "is based on a physically observable property of the molecule" rather than on the mathematical wave function Ψ. In a reply to his review [28], it is pointed out that the sole purpose of the wave function is a means to an end, to enable the prediction of measurable quantities which are subsequently understood in terms of the theorems that relate them to the forces acting within the system, a view espoused by Schrödinger and admirably demonstrated by Slater. This is the approach to be followed in this article. It will be contrasted with the interpretations presented by Frenking et al. [24,25] that are couched in terms of orbitals, as exemplified in the use of orbitally based analyses of populations and other properties and the energy partitioning schemes of Morokuma [29] and of Ziegler and Rauk [30].

Macchi and Sironi [31] have presented an analysis of bonding in transition metal carbonyl complexes using QTAIM in conjunction with orbital models applied to both experimental and theoretical densities. Their study focuses on metal–metal bonding in polynuclear carbonyl complexes, as well as metal carbonyl bonding including the three carbonyl complexes reported on here. Their presentation of the data obtained from the bond indices derived from a QTAIM analysis is comprehensive, data that emphasises the unique properties associated with transition metal bonding. Their discussion is however, melded with rather than distinguished from associated orbital analyses. The present paper complements their work on the QTAIM analysis of the carbonyl complexes and significantly extends their interpretation of metal–carbon bonding.

3. Calculations

The Kohn–Sham implementation of density functional theory (DFT) [32] gives superior binding energies and geometries relative to comparable restricted Hartree–Fock (HF) calculations for transition metal complexes. The $Cr(CO)_6$ molecule for example, is not bound relative to the separated reactants at HF [33], while Ziegler et al. [34] obtain a binding energy in agreement with experiment using DFT. The B3LYP formulation of Kohn–Sham theory, as incorporated in GAUSSIAN98, is employed in 6-311+G(2d)//6-311+G(2d) calculations for all systems. Macchi and Sironi (M&S) [31] employ the same procedure in their work, using comparable basis sets, employing a relativistic effective core potential for the metal atoms. In line with the known insensitivity of QTAIM properties to basis set, their calculated atomic prop-

erties and bond indices do not exhibit any significant differences from those reported here (M&S values bracketed); the two sets of results for $Cr(CO)_6$ yielding, for example, q(Cr) = 1.13e (1.16e), $\rho_{b(Cr–C)}$ = 1.06 au (1.06 au), $\nabla^2\rho_{b(Cr–C)}$ = 0.475 au (0.461 au). Persson and Taylor [35] have performed large basis set coupled cluster calculations on the three carbonyl complexes and obtain agreement with the experimental binding energies for $Fe(CO)_5$ and $Ni(CO)_4$ but their value of 164 kcal/mol is in disagreement with the published experimental result of 156 kcal/mol for $Cr(CO)_6$, a result they question.

The calculated energies and bond lengths and the comparison with the relevant experimental values are given in Table 1. The metallocenes are in the staggered D_{5d} geometry. The Ge complex is calculated to be 1.2 kcal/mol more stable in the 'bent' geometry [36]. Also included are the sums of the integrated atomic energies and populations and their differences from the molecular values. The small differences indicate that the errors in the atomic integrations are negligible. The calculated binding energies ΔE, compared to the results of Persson and Taylor, are in error by 5, 21 and 11% for the Cr, Fe and Ni complexes.

4. Atoms and structure defined by the measurable density

4.1. Atoms of QTAIM and their relation to chemistry

QTAIM defines an atom in a molecule as a region of space bounded by a surface $S(r)$ that exhibits the property of 'zero-flux', meaning that $S(r)$ is not crossed by any gradient vectors of the electron density $\rho(r)$. This condition is expressed in Eq. (1), where $n(r)$ represents a unit vector perpendicular to the surface,

$$\nabla\rho(r)\cdot n(r) = 0 \quad \text{for every point } r \text{ on the surface } S(r) \tag{1}$$

This zero-flux condition, one that is both defined and measurable in real space, serves a dual purpose: it defines the boundary condition for the application of quantum mechanics to an open system – to an atom in a molecule – and its application to a molecular charge distribution yields an exhaustive partitioning of the molecule into non-overlapping atoms. Because of these dual consequences, the atoms of theory possess the characteristics that are essential to the understanding and prediction of molecular properties: (i) Every property expressible as the expectation value of a Dirac observable, is defined for an atom in a molecule and every property makes an additive contribution to the molecular expectation value. (ii) The atoms and functional groups defined within QTAIM maximise the transferability of properties from one molecule to another. This follows from the truism that two pieces of matter or two atoms, are identical only if they possess identical charge distributions. Since an atom of theory is defined by its charge distribution as a bounded region of real space, its form necessarily reflects its properties. Recent work, both experimental [37–41] and theoretical [42], has demonstrated the remarkable transferability of the charge distributions and properties of the main-chain and other functional groups common to the amino acids and of their side-chains when the amino acid is bound as a residue in a tripeptide [43]. (iii) Atomic and group properties always sum to the observed molecular

Table 1
Calculated energies and geometries of complexes[a,b]

	E	ΔE[c]	R(M–C)[c]	R(C–O)/R(C–C)[c]	$-V/T$	$\sum_\Omega E(\Omega) - E$	$\sum_\Omega N(\Omega) - N$
Complex							
$Cr(CO)_6$	−1724.79293	−155 (153)[1]	3.643 (3.608)[5]	2.153 (2.149)[3]	2.002175	0.027	0.0048
$Fe(CO)_5$	−1830.63517	−166 (137)[2]	ax 3.459 (3.413)[6]	2.149	2.001855	0.001	0.0043
			eq 3.444 (3.464)[6]	2.156 (2.164)[6]			
$Ni(CO)_4$	−1961.86334	−123 (138)[3]	3.489 (3.477)[7]	2.156 (2.173)[7]	2.001588	0.301	0.0049
$Fe(Cp)_2$	−1650.90204	−170 (146)[4]	3.934 (3.842)[8]	2.687 (2.625)[8]	2.001840		0.0002
$Al(Cp)_2^+$	−629.39120	−124	4.120 (4.072)[9]	2.691	2.003868	0.147	0.0061
$Ge(Cp)_2$	−2464.16303	−129	4.886 (4.772)[10]	2.673 (2.625)[10]	2.001995		0.0055
Ligand							
CO	−113.35352			2.127			
				(2.132)	2.004000	0.205	0.0032
$Cp^\bullet$	−193.51408			2.655	2.004953	0.053	0.0005
Cp^-	−193.57771			2.667	2.005025	0.040	0.0001

(1) D.A. Pittam, G. Pilcher, D.S. Barnes, H.A. Skinner, D. Todd, J. Less-Common Met. 42 (1975) 217. (2) R.H. Shultz, K.C. Crellin, P.B. Armentrout, J. Am Chem. Soc. 113 (1991) 8590. (3) L.S. Sunderlin, D. Wang, R.R. Squires, J. Am. Chem. Soc. 114 (1992) 2788. (4) V.I. Tel'noi, I.B. Rabinovich, Russ. Chem. Rev. 46 (1977) 689. (5) J. Whintaker, J.W. Jeffery, Acta Crystallogr. 23 (1967) 977. (6) B. Beagley, D.W.J. Cruickshank, P.M. Pinder, A.G. Robiette, G.M. Sheldrick, Acta Crystallogr. B25 (1969) 737. (7) J. Ladell, B. Post, I. Fankuchen, Acta Crystallogr. 5 (1952) 795. (8) P. Seiler, J.D. Dunitz, Acta Crystallogr. B35 (1979) 1068. (9) C. Dohmeir, D. Loos, H. Schnöckel, Angew. Chem. Int. Ed. Engl. 35 (1996) 129. (10) S.P. Constantine, H. Cox, P.B. Hitchcock, G.A. Lawless, Organometallics 19 (2000) 317.

[a] B3LYP/6-311+G(2d).

[b] E and R in atomic units, ΔE and $\sum_\Omega E(\Omega) - E$ in kcal/mol.

[c] Experimental values in parenthesis.

value and are always in agreement with experimentally determined values, as has been demonstrated for heats of formation, molar volumes and electric and magnetic susceptibilities in molecules that exhibit group additivity [44–46]. The chemical relevance of the theory is further demonstrated in the recovery of measured differences in group properties ascribed to strain energy, resonance energy and aromatic magnetic exaltation [47]. Agreement with observation is the only test of theory [48].

4.2. Molecular and virial graphs

In a bound molecular state, the nuclei of bonded atoms are linked by a line along which the electron density is a maximum with respect to any neighbouring line; they are linked by a *bond path* [49,50]. The resulting *molecular graph*, the linked network of bond paths that defines a system's molecular structure, has been shown to recover the 'chemical structures' in a multitude of systems, in terms of densities obtained from both theory [51] and experiment [52], structures that were previously inferred from classical models of bonding in conjunction with observed physical and chemical properties. The gradient vector field of the electron density for $Cr(CO)_6$ is displayed in Fig. 1. The topology of this field defines the atomic basins, their boundaries and the bond paths [1,53]. An accompanying diagram shows the superposition of the atomic boundaries and bond paths defined by the gradient vector field on the electron density distribution.

The physical presence of bonding between atoms also signifies an accompanying energetic stabilisation, since every bond path is mirrored by a *virial path* linking the same nuclei along which the electronic potential energy density is maximally stabilising [54]. Thus, co-existing with every molecular graph, is a shadow graph – the virial graph – indicating the presence of a corresponding set of lines, again defined in real space, that delineates the lowering in energy associated with the formation of the structure defined by the molecular graph [55]. The presence of a bond path always implies stabilisation, even when present in cases where classical models invoke 'steric repulsions', as is done to account for the stabilisation of the tetrahedrane and cyclobutadiene molecules through their corseting by *tert*-butyl groups. The stabilisation of these molecules is not the result of 'non-bonded repulsions' between the methyl groups, however that might lead to their stabilisation, but is rather a consequence of the enveloping of the central C_4 systems by H–H bond paths linking the methyl

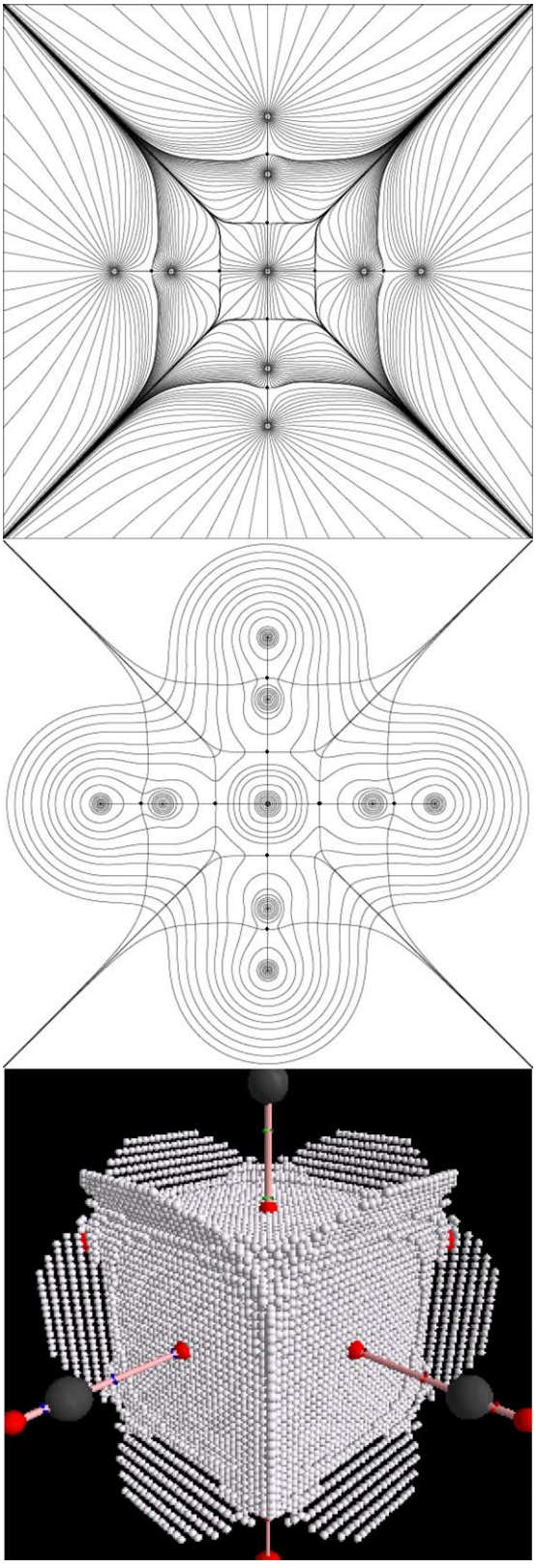

Fig. 1. Displays of the gradient vector field and of the electron density in a symmetry plane of $Cr(CO)_6$. The density map is overlaid with the atomic boundaries and bond paths defined by trajectories that terminate and originate respectively, at bond critical points (CPs) in the gradient vector field, points marked by dots in both fields. An atomic basin is defined by the set of trajectories that terminate at its nucleus or, alternatively, by the interatomic surfaces it shares with its bonded neighbours. Three of the six surfaces bounding the Cr atom are shown in the lower diagram. All of the properties of this enclosed region are defined and they make additive contributions to the properties of the complex. It is shown that the principal source of bonding in $Cr(CO)_6$ is the electrostatic interaction of the Cr atom density with the nuclei of the ligands. The outer contour value is 0.001 au and the remaining contours increase in value in the order 2×10^n, 4×10^n, 8×10^n au with n beginning at -3 and increasing in steps of unity.

groups of neighbouring *tert*-butyl groups [56]. Rupturing this encasing network of bond paths requires energy, as does the rupturing of any bond path, an energy that in the case of tetra-*tert*-butyl cyclobutadiene, is in excess of 50 kcal/mol. Those who doubt the universal identification of a bond path with bonding citing the presence of bond paths between anions in an ionic crystal for example, should differentiate between classical models of bonding and its proper quantum mechanical description [49,57].

The molecular graphs and their complementary homeomorphic virial graphs for the molecules in this study are shown in Figs. 2 and 3. They recover the anticipated 'chemical structures' for the metal carbonyl complexes $M(CO)_n$. The molecular graphs for $M(Cp)_2$ show that the Al, Fe and Ge are linked by bond paths to each of the carbon atoms of the Cp rings; they are $(\eta^5\text{-Cp})_2M$. The bonding defined in these graphs is the subject of this paper.

5. Characterisation of metal–ligand bonding in terms of pair and bond indices

5.1. Counting the number of localised and shared electron pairs

The molecular graphs for the MCp_2 molecules require comment. The chemical structures of a metal atom bonded to an unsaturated ring are sometimes denoted by 'bonds' linking M to each carbon of the ring and at other times, by a single 'bond' linking the metal atom to the centre of the unsaturated ring. The cyclopentadienyl complexes are electron deficient molecules in the Lewis sense. Moffit, in his pioneering molecular orbital study of the bonding in $FeCp_2$, argued that the bonding of a Cp ring to the iron atom depicted by five 'bonds' is a result of the participation of two pairs of electrons [58]. Neither a bond in a chemical structure nor a corresponding bond path necessarily implies the sharing of one or more Lewis electron pairs. QTAIM however, does provide an answer to the problem of counting the number of electrons shared between pairs of atoms and the number localised on each.

We begin with a 1954 quotation from Lennard-Jones: "Electrons of like spin tend to avoid each other. This effect is more powerful, much more powerful than that of the electrostatic forces. It does more to determine the properties and shapes of molecules than any other single factor. It is the exclusion principle which plays the dominant role in chemistry" [59,60]. He demonstrated that the most probable relative positions assumed by two, three and four same spin electrons are a direct consequence of the *space correlation function*, the pair density for same-spin electrons [61]. The results of his studies provided the basis for the rules embodied in the VSEPR model of molecular geometry [62,63]. Unfortunately, the understanding of electron pairing and its spatial localisation afforded by the pair density was suppressed and its function replaced by the use of localised molecular orbitals. *Individual orbitals, however defined, provide no information regarding the spatial pairing or localisation of electrons*. Instead, these properties, as demonstrated in the pioneering papers of Lennard-Jones, are determined by the pair density, and are best understood in terms of the conditional same spin density [64,65].

The conditional same spin density $\delta^{\alpha\alpha}(r_1, r_2)$, Eq. (2), determines the extent to which the exclusion principle decreases the density of an α electron at some position r_2 when another α electron has the position coordinate r_1. It is obtained by dividing the α-spin pair density by $\rho^{\alpha}(r_1)$, the spin density for one of the electrons, a similar expression holding for the β electrons.

$$\frac{\rho^{\alpha\alpha}(r_1, r_2)}{\rho^{\alpha}(r_1)} = \delta^{\alpha\alpha}(r_1, r_2) = \left[\rho^{\alpha}(r_2) + h^{\alpha\alpha}(r_1, r_2)\right] \quad (2)$$

It must be understood that neither electron is fixed at either of these points, the charge of each being spread out in space in the manner determined by the spin density $\rho^{\alpha}(r)$. The quantity $h^{\alpha\alpha}(r_1, r_2)$ describes the density of the Fermi hole. It equals the exchange density for α-spin electrons divided by $\rho^{\alpha}(r_1)$. It is a negative quantity that describes the extent to which the density of the second electron is excluded from the neighbourhood of r_1 [66]. The integral of $h^{\alpha\alpha}(r_1, r_2)$ over r_2 equals –1, corresponding to the removal of one α-spin electron. The exclusion is locally complete for $r_1 = r_2$, since $h^{\alpha\alpha}(r_1, r_1) = -\rho^{\alpha}(r_1)$. If $h^{\alpha\alpha}(r_1, r_2) \sim -\rho^{\alpha}(r_2)$ for positions removed from r_1, that is, the density of the Fermi hole is *localised* about this point, then all other α-spin electrons will be excluded from the space corresponding to the exclusion of one electronic charge. In a closed-shell system, the Fermi hole density of an electron of β-spin will be similarly localised, resulting in a pair of electrons being localised about the point r_1. If on the other hand, the density of the Fermi hole is diffuse, then the exclusion of same spin electrons occurs over an extended region of space and the electron is *delocalized*. One has the simple understanding that if the exchange of electrons is largely confined to within a given atomic basin, then the electrons are correspondingly localised on that atom, while if the electrons exchange between atomic basins, then the electrons are delocalized over both atoms or, equivalently, are shared by both atoms. *Thus, the physical picture underlying electron delocalization is exceedingly simple—it is determined by the extent to which the electrons on one atom exchange with those on another*.

The Fermi correlation for all α electrons is obtained by multiplying the density of the Fermi hole by the spin density to yield the exchange density, the quantity $\rho^{\alpha}(r_1)\, h^{\alpha\alpha}(r_1, r_2)$. From this point on, we shall assume a closed-shell system and all results refer to integration over both sets of spins. The total Fermi correlation is obtained by the integration of the exchange density over the coordinates of both electrons, a quantity that equals $-N^{\alpha} - N^{\beta} = -N$. That is, the exchange density removes a total of N electrons from the expression for the pair density to yield $(1/2)(N^2 - N) = (1/2)N(N - 1)$ pairs. The total Fermi correlation contained within a single

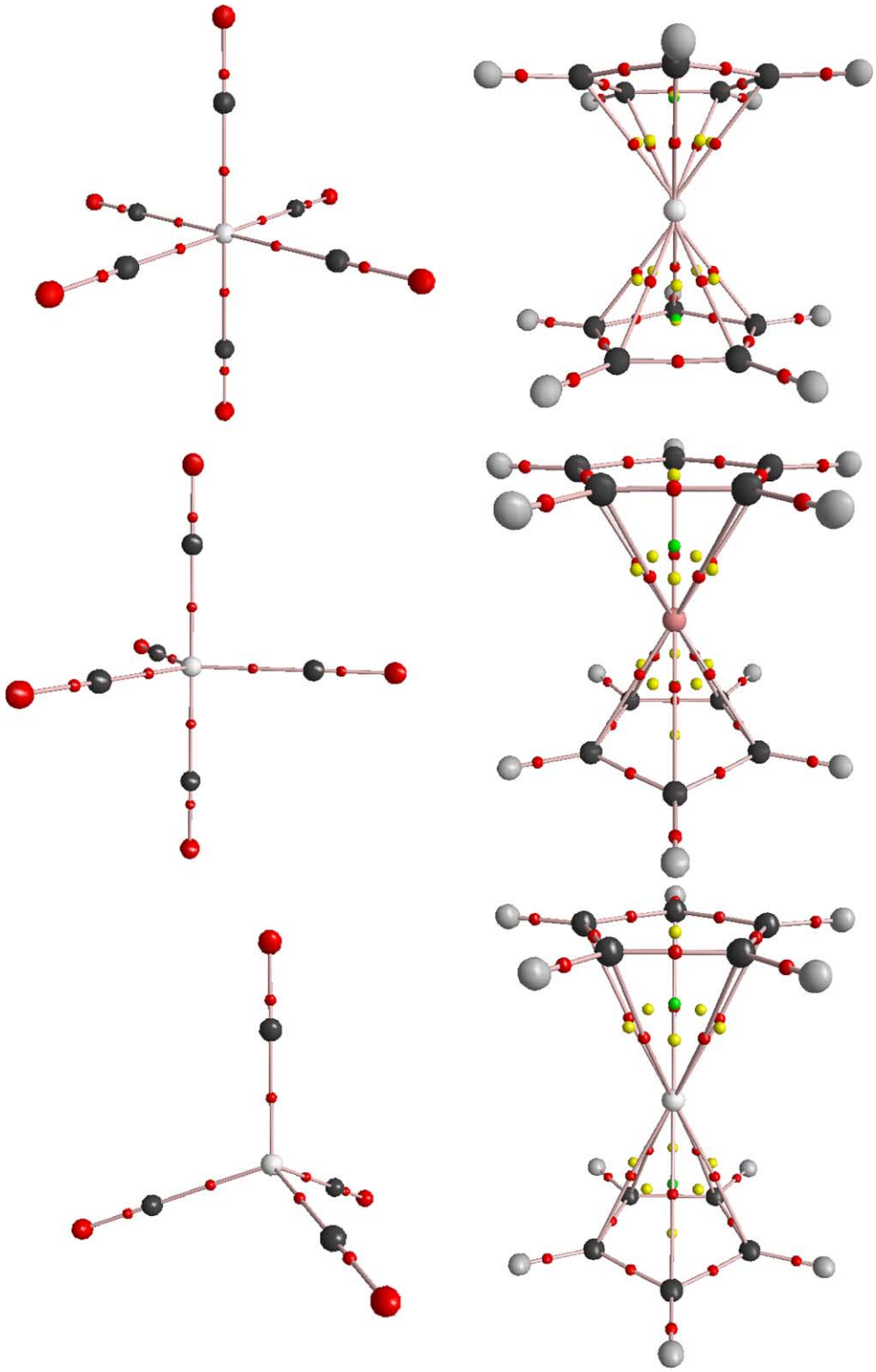

Fig. 2. Molecular graphs of the carbonyl complexes of Cr, Fe and Ni in descending order on the left, and of the metallocenes of Fe, Al^+ and Ge on the right. The colour scheme identifying the critical points is as follows; red for (3, −1) or bond CP; yellow for (3, +1) or ring CP; green for (3, +3) or cage CP. The nuclear maxima, denoted by larger spheres, are: red for oxygen; black for carbon; white for hydrogen. The alternating bond and ring CPs resulting from the bonding of M to the carbons in the metallocenes denote a ring of almost constant density and a corresponding delocalisation of the bonding density over the ring surfaces.

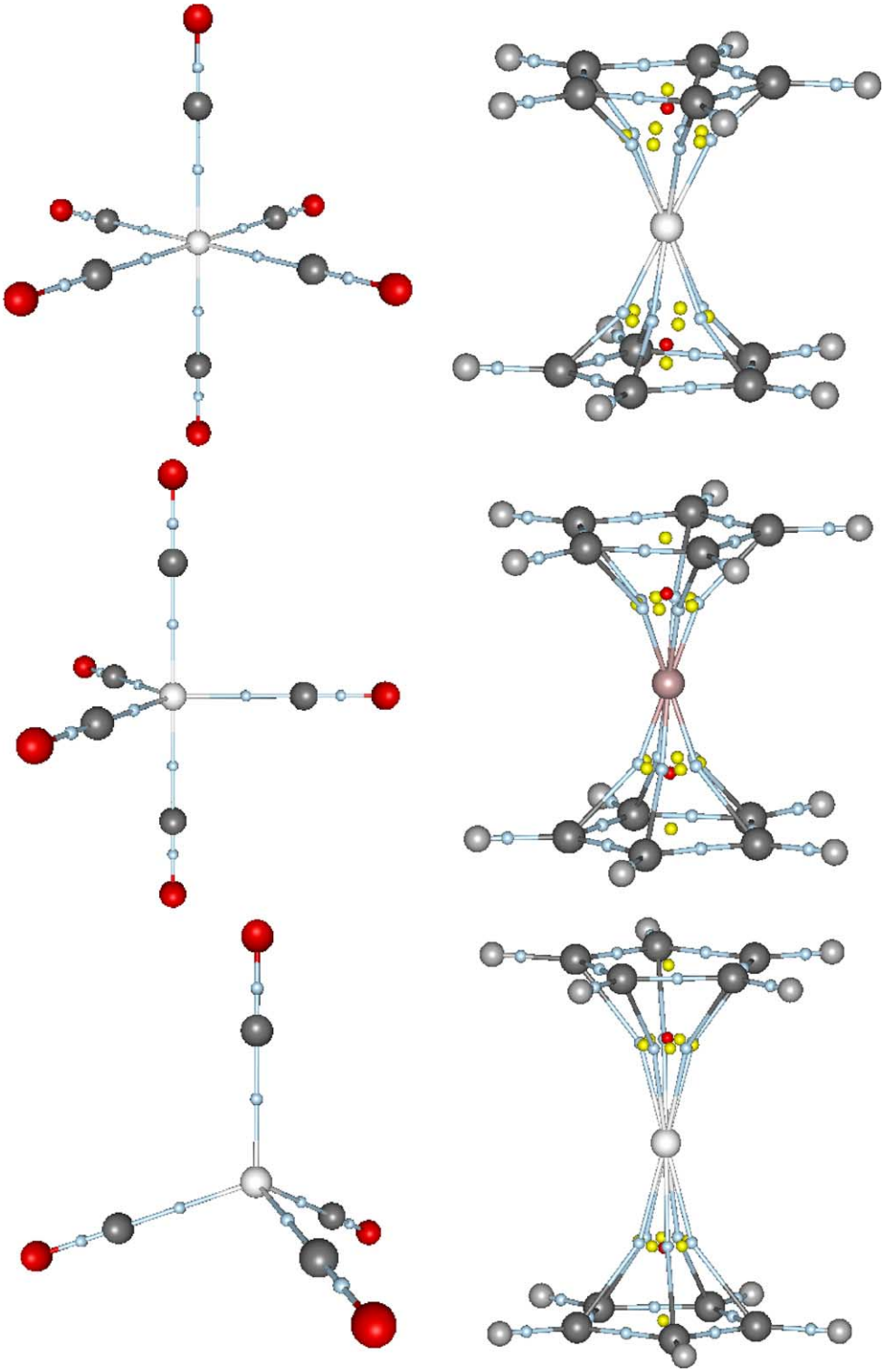

Fig. 3. Virial graphs of the carbonyls and metallocenes in same order as in Fig. 2. Every CP in the molecular graph is mirrored by a corresponding CP in the virial graph and associated with every bond path is a virial path, a line of maximally stabilising potential energy. The colour scheme identifying the critical points is as follows; blue for (3, −1) or virial path CP; yellow for (3, +1) or ring CP; red for (3, +3) or cage CP.

atom A, the quantity F(A, A), is obtained by integration of the exchange density over its basin and for a HF or single determinant wave function, the result is expressible in terms of the overlap of all pairs of orbitals over the basin of the atom [66],

$$F(\mathrm{A},\mathrm{A}) = -\sum_{i,j} S_{ij}^2(\mathrm{A}) \tag{3}$$

$|F(\mathrm{A},\mathrm{A}) = \lambda(\mathrm{A})|$, the *electron localisation index* for atom A, determines the number of electrons localised to the basin of atom A. Its limiting value is clearly N(A), the population of atom A, in which case one would have N(A)/2 pairs of electrons localised on A, with all other α and β electrons being excluded from A. While this limiting situation is obtained only for an isolated atom, it is closely approached in ionic systems such as NaCl, where $l(\mathrm{A}) = \lambda(\mathrm{A})/N(\mathrm{A}) \times 100\%$, the *percent localisation* of the electrons on A, can approach 99%.

The delocalization of electrons between two atomic basins A and B is given by the corresponding expression F(A, B), Eq. (4) [66],

$$F(\mathrm{A},\mathrm{B}) = -\sum_{i,j} S_{ij}(\mathrm{A}) S_{ij}(\mathrm{B}) \tag{4}$$

F(A, B) equals F(B, A) and the magnitude of their sum, the delocalization index δ(A, B), is a measure of the extent of exchange of the electrons of A with those of B [67]. The sum of F(A, A), F(A, B) and F(B, A) over all atoms in a molecules equals $-N$ and thus all electrons are accounted for. In particular, one has

$$N(\mathrm{A}) = \lambda(\mathrm{A}) + \left(\frac{1}{2}\right) \sum_{\mathrm{B}\neq\mathrm{A}} \delta(\mathrm{A},\mathrm{B}) \tag{5}$$

an equation that determines the fraction of the electron population of A that is localised on A and the fraction shared with or delocalized over the basins of other atoms. Similar equations apply at all levels of theory. One notes that the definitions of λ(A) and δ(A, B) involve sums over all pairs of orbitals and they are therefore, independent of any unitary transformation of the orbitals – all sets, localised or canonical – yield the same answers.

5.2. Distinguishing between an electron pair and a population of two

The average number of electron pairs contained within a region A, the quantity D_2(A, A), is given by [1,66]

$$D_2(\mathrm{A},\mathrm{A}) = \frac{[N(\mathrm{A})^2 + F(\mathrm{A},\mathrm{A})]}{2} \tag{6}$$

It is important to understand the distinction between an average *electron population* of two for some region A, N(A) = 2, as determined by integration of the electron density, and a *pair of electrons* localised to A, D_2(A, A) = 1, as determined by integration of the pair density. A display of the density of a doubly occupied orbital cannot be interpreted as a display of an 'electron pair'. Denote the space occupied by 99.9% of the density of two electrons in orbital ϕ_i by A, as pictured in displays of the density of say, a bonded or non-bonded localised orbital. Only if no other orbitals were to contribute density to the region A, that is, only if there is no overlap of orbital ϕ_i with any other orbital, will the two electrons in A be a localised pair. In the instance of no overlap, F(A, A) reduces to $-2S_{ii}^2(\mathrm{A}) = -2$, corresponding to the exclusion of all other electrons from A. Since N(A) = 2, the number of pairs in A is, from Eq. (6), equal to one. This situation is not obtained nor even approached for valence orbitals. For any finite region A with an average population of two, no single orbital will have an overlap of unity and all other S_{ij}(A) = 0, although this situation can be approached for a core orbital. In NaCl for example, D_2(Na, Na) = 45.9, a value 0.9 in excess of five localised pairs of electrons. *No valence orbital occupies its own region of space, the requirement for the localisation of an electron pair*. As a result, $|F(\mathrm{A},\mathrm{A})|$ is necessarily decreased from its value of 2 and more than a single pair of electrons contributes to the density in A. Thus, even if a region of space has an average population of two, a number of pairs will in general contribute to that region and it is not a localised electron pair. *A display of the density of a localised orbital is just that—a display of that orbital's contribution to the total density. It is not a display of an'electron pair*'. Localised orbitals are not that localised and they are not localised to separate regions of space, exhibiting substantial values for their absolute overlap [68]. The identification of the density of a localised orbital with an 'electron pair' is amongst the most common of the misuses of the orbital model.

5.3. Recovery of the Lewis model in the delocalisation indices

A single determinantal wave function provides the theoretical personification of the Lewis electron pair model with the delocalisation index providing a measure of the bond order between bonded atoms [67]. A DFT calculation does not possess a second-order density matrix [69a]. The B3LYP functional however, calculates the exchange density using the DFT orbitals in the restricted Hartree–Fock (RHF) expression for exchange, and the use of Eqs. (3) and (4) yields indices that while, somewhat larger than the RHF values, provide a meaningful measure of electron delocalisation [69b]. For example, the values of δ(M, C), the delocalisation of the metal atom onto C of CO, exceed the RHF values by 9%.

The equal sharing of one Lewis pair between A and B requires that λ(A) = λ(B) = 0.5 and δ(A, B) = 1.0 and hence δ(A, B) = 1, 2 or 3 for the corresponding numbers of shared pairs of electrons. If the sharing of a pair is accompanied by a transfer of electronic charge from A to B, then the localisation of the density in the atomic basins increases and δ(A, B) < 1.0, assuming values <0.2 for ionic interactions. Austen has shown that the value of δ(A, B) for an A–B molecule with charge transfer decreases from values of one, two and three,

as a function of the square of the transferred charge [70]. Thus, a value of δ(A, B) < 1 for a pair of atoms linked by a bond path does not imply that less than a pair of electrons is shared between A and B, but that they are unequally shared. In addition, δ(A, B) is somewhat less than unity for an equally shared pair between two atoms in a polyatomic molecule, since the electrons on A and B are further delocalised over other atoms in the system, δ(C, C) = 0.99 and 1.89 for the C–C bonding in ethane and ethylene, for example. In any case, the value of δ(A, B) always gives the number of electrons that are delocalised or exchanged between the basins of A and B, independent of any model. In addition to the percent localisation index l(A), it is useful to define the difference $\Delta(A) = N(A) - \lambda(A)$, one that determines the number of electrons of A delocalised into the basins of other atoms.

The exchange of one or more pairs of electrons between bonded atoms is the mechanism essential to the notion of 'covalent bonding'. Thus, the delocalisation index δ(A, B), since it determines the number of pairs exchanged between two atomic basins, may be used to gauge the degree of covalency. In the theory of atoms in molecules 'covalency' is replaced with the term 'shared interaction', one that invokes the role of sharing, i.e., the exchange of electrons between bonded atoms. What is important is that the delocalisation index, defined as the expectation value of the exchange operator over two atomic basins, provides a quantitative measure of the number of electrons exchanged in any given interaction thus quantifying 'covalency' for those who wish to retain the term.

5.4. Electron sharing in carbonyls and metallocenes

Table 2 gives the values of l(A), Δ(A) and δ(A, B) for the carbonyl and Cp complexes, the former being discussed first. There is a transfer of electronic charge from the metal atom M to each carbon atom amounting to 0.19, 0.15 and 0.13e for the Cr, Fe and Ni complexes, respectively. There is also a much smaller a transfer of electronic charge, ∼0.03e, to each carbon from oxygen. The most important observation concerning the carbonyl complexes is the significant degree of delocalisation between the metal and the carbon atoms, with δ(M, C) values clustered around unity, indicating a close to equal sharing of one Lewis pair between M and each of the C atoms. The values of l(M) are ∼90% because of the essentially complete localisation of the 18 electron cores on each metal, values determined by the atomic overlap matrix. The valence density is less localised, being 40, 59 and 76% localised on the Cr, Fe and Ni atoms, respectively. The quantity Δ(M), giving the number of electrons of the metal that are delocalised onto the remaining atoms, amounts to 2.9, 3.0 and 2.3e, respectively, for Cr, Fe and Ni, ∼86% of which are delocalised onto the carbon atoms in each case. The relatively small charge transfer per ligand carbon atom is consistent with the nearly equal sharing of the density delocalised between M and each C. The delocalisation of the metal electrons onto the oxygens is smaller by a factor of 0.2. An important observation is the decrease in the localisation of the density of the carbon atom, from a value of l(C) = 81% in free CO to values of ∼70% in the complexes. This is not simply the result of each carbon being in the presence of an increased number of atoms – the localisation of the density on each oxygen undergoes a decrease of only 1% on complex formation – but is rather the result of the significant delocalisation, i.e., sharing, of the density between each carbon and the metal atom. This is accompanied by a decrease of ∼0.2 in the value of δ(C, O) from its uncomplexed value that is accompanied by a C–O bond lengthening of 0.02 au. The values of non-bonded indices, δ(C′, O′) and δ(O, O′), are all 0.01 or less.

The metal atoms in the metallocenes transfer electronic charge to each carbon of the Cp rings, in amounts of 0.14, 0.09 and 0.08e in the Al^+, Ge and Fe complexes, respectively. The extent of delocalization of the metal atom electrons onto the carbons of the Cp rings, the values Δ(M), increase in the reverse order, Al^+ < Ge < Fe, with a maximum value of 2.4 for Fe compared to 3.0 in its carbonyl complex. The total number of electrons exchanged between M and the carbons of the rings is simply 10 × δ(M, C) which equals 1.3, 2.5 and 4.5 for the Al, Ge and Fe complexes respectively. The value of 4.5 for ferrocene translates into the exchange of just over two Lewis electron pairs with each ring, compared with Moffit's model of two bonding pairs [58]. The

Table 2
Electron localization and delocalization indices[a]

Complex	l(M)	l(C)	l(O)	Δ(M)	Δ(C)	Δ(O)	δ(M, C)	δ(M, O)	δ(C, O)	δ(C, C′)
$Cr(CO)_6$	87.27	70.66	89.71	2.91	1.49	0.94	0.8255	0.1418	1.6286	0.0982
$Fe(CO)_5$										
ax	88.15	69.55	89.72	2.99	1.52	0.94	0.9800	0.1668	1.6231	0.0510
eq		69.48	89.68		1.54	0.94	1.0532	0.1781	1.6140	0.0244
$Ni(CO)_4$	91.74	71.36	89.77	2.27	1.43	0.93	0.9763	0.1585	1.6585	0.0637
	l(M)	l(C)	l(H)	Δ(M)	Δ(C)	Δ(H)	δ(M, C)	δ(M, H)	δ(C, C′)	δ(C, C″)
$Fe(Cp)_2$	90.67	65.87	42.15	2.35	2.10	0.53	0.4518	0.0182	1.2480	0.0792
$Al^+(Cp)_2$	93.91	66.69	39.54	0.65	2.09	0.52	0.1272	0.0024	1.3416	0.1374
$Ge(Cp)_2$	95.85	65.64	43.40	1.29	2.10	0.56	0.2486	0.0100	1.3026	0.1060

[a] Values for ligands: CO: l(C) 81.31, l(O) 90.08, δ(C, O) 1.8104. Cp^- l(C) 66.44, l(H) 44.58, δ(C, C′) 1.3852, δ(C, C″) 0.1329.

values of δ(C–C) between bonded and nearest neighbour carbons in the Cp rings of the complexes approach the values of 1.39 and 0.13 found in the cyclopentadienyl anion, a consequence of the transfer of electrons from the metal atom to the rings.

5.5. Characterisation in terms of bond critical points

The bond critical point (BCP) data is given in Table 3. Macchi and Sironi [31] give a comprehensive discussion of the BCP properties for metal carbonyls and for metal–metal bonding. Their discussion is prefaced with a summary of BCP properties for prototype molecules representing the full range of atomic interactions and concludes with a summarising table of the features that serve to characterise the types bonding between 'light' as opposed to 'heavy' (metal) atoms. The present discussion is thus limited to the essential features that characterise the bonding in the metal complexes.

The delocalisation indices for M–C bonding in the carbonyls are typical of shared interactions, a view consistent with the property values at the M–C bond CP. The values of ρ_b for the carbonyls, while at the low end for shared interactions, are significantly larger than those associated with a closed-shell interaction. The still smaller values of ρ_b found for the M–C bonding in the Cp complexes are a reflection of the delocalisation of the density over the multiple links between the metal atom and the carbons of the rings. The energy density H_b is negative, as typical for a shared interaction [71], but smaller than that for a singly bonded shared interaction and the ratio G_b/ρ_b, where G_b is the kinetic energy density, equals ~1.4 while it is <1.0 for shared interactions. The M–C interatomic surface for all the metal interactions falls in the region of the outer shell of charge depletion of the metal atom imparting to metal bonding and post transition atoms up to the metalloids (up to the element arsenic in the fourth row) a unique set of characteristics, among them being a necessarily positive value for $\nabla^2\rho_b$. This combination of BCP indices; relatively low values for ρ_b, small negative values for H_b with $G_b/\rho_b \sim 1$ and small positive values for values $\nabla^2\rho_b$, coupled with significant electron delocalisation, are unique to bonding to a metal atom [5,72,31]. Another characteristic feature is the planarity of the metal–carbon interatomic surface, evident in Fig. 1 for the Cr–C surface, but found for Fe–C and Ni–C surfaces as well. The electron delocalisation indices for metal–metal bonding can be characteristic of single or multiple bonds, the Ga–Ga interaction in the dianion $[HGaGaH]^{2-}$ for example, in addition to exhibiting the above characteristic BCP values, has a δ(Ga, Ga) value of 2 [5]. There is a decrease of 0.02 au in the value of ρ_b for C–O upon complexation, with $\nabla^2\rho_b$ decreasing by ~0.1 au, changes commensurate with the slight increase of ~0.02 au in the bond length.

Table 3
Bond critical point data in atomic units

	ρ_b	$\nabla^2\rho_b$	G_b	H_b	G_b/ρ_b	r_b(M)	r_b(C)
M–CO							
$Cr(CO)_6$	0.1059	0.4745	0.1473	−0.0287	1.3909	1.7968	1.8466
$Fe(CO)_5$							
ax	0.1300	0.5403	0.1799	−0.0448	1.3838	1.7059	1.7527
eq	0.1399	0.4959	0.1782	−0.0542	1.2738	1.7617	1.6823
$Ni(CO)_4$	0.1264	0.5037	0.1688	−0.0428	1.3354	1.7586	1.7304
M–Cp							
$Fe(Cp)_2$	0.0826	0.2720	0.0888	−0.0208	1.0751	1.9491	1.9900
$Al(Cp)_2^+$	0.0501	0.1635	0.0538	−0.0129	1.0739	1.6311	2.4887
$Ge(Cp)_2$	0.0355	0.0755	0.0224	−0.0035	0.6310	2.4053	2.4822

5.6. Surface delocalization in bonding to an unsaturated ring

The linking of the metal atoms to carbons of the Cp rings results in the formation of three-membered rings and a (3, +1) or ring CP is present in the face of each ring, the point where the density attains its minimum value in the ring surface, Fig. 2. There is a ring CP in the centre of a Cp ring as well, and this ring surface, together with the five surfaces formed by the links to the metal atom, define a cage enclosing a (3, +3) or cage CP. Each three-membered ring CP lies on a line linking the neighbouring BCPs, Fig. 2, and it has a value, ρ_r, that is only 0.002 au or less than ρ_b which possesses the lowest value of the density along the perimeter of each ring, a feature most clearly seen in the diagram for the Al^+ complex. The result is a ring of almost constant density girdling each cage, defined by the alternating set of bond and ring CPs with a value of 0.082 ± 0.001 for Fe, 0.050 ± 0.001 for Al and 0.035 ± 0.001 for Ge. Thus, the bonding of a metal atom to an unsaturated ring is not well represented in terms of a set of individual bond paths, but rather by a bonded cone of density, with the density at any point on an individual bond path having a value only slightly in excess of that for points displaced off the bond path into the faces of the neighbouring rings, as depicted for ferrocene in Fig. 4. Clearly, the interaction of a metal atom with a Cp ring is best viewed as involving an interaction with the delocalized density of the entire ring perimeter, a picture that is conceptually similar to that used to denote the interaction of a metal with an unsaturated ring in a conventional structure diagram. The delocalization indices indicate that two pairs of electrons are shared between Fe and each Cp ring and the result is an enhanced binding over what one would anticipate on the basis of the individual ρ_b values.

This view of metallocene bonding was previously put forth in the description of the interaction of titanium with a Cp ring [73], where it is shown that the surface delocalisation of the density accounts for the facile rotation of the Cp ring in metallocenes. The delocalization of the bonding density over ring surfaces is characteristic of electron deficient systems as found for example, for the surfaces of three- and four-membered rings formed by the boron and/or carbon atoms in boranes and carboranes, as previously documented [74].

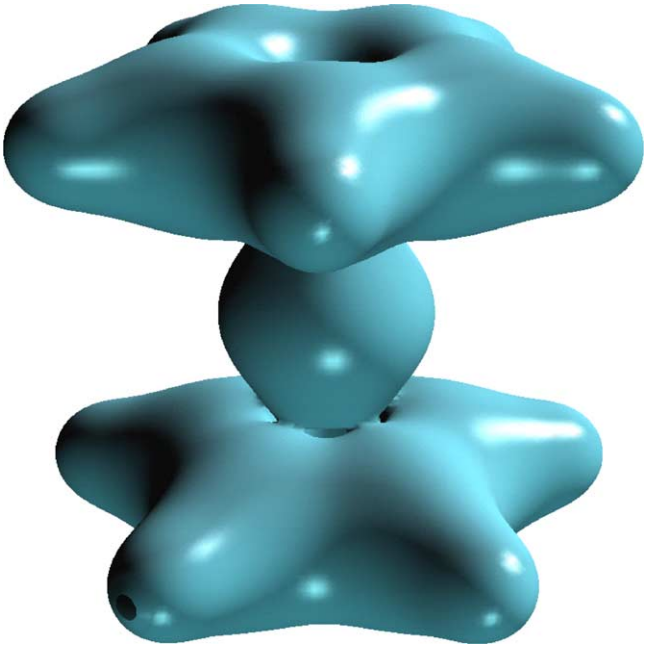

Fig. 4. An envelope of the density for ferrocene with a value for the density equal to the average value of the bond and ring critical points associated with the Fe–C bonding that are displayed in Fig. 2.

6. Origin of bonding energy

6.1. Bonding energy in terms of changes in energy expectation values

The sole stabilising *force* in the formation of a molecule is the electrostatic attraction of the nuclei for the electron density, the corresponding contribution to the potential energy being labelled V_{en}. Countering this are the electrostatic repulsions, electron–electron, V_{ee}, and nuclear–nuclear, V_{nn}. V_{nn} is a purely classical term and V_{ee} is comprised of the classical Coulomb repulsion, expressible in terms of the density as the double integral of $(1/2)\rho(r_1)\rho(r_2)/r_{12}$, and the exchange energy, a uniquely quantum mechanical entity. The exchange of same-spin electrons plays a role well beyond the reduction in the Coulomb repulsion between the electrons [59], determining the spatial delocalization and spatial pairing of electrons [66], two quantities that play a central role throughout chemistry, as illustrated here in the quantum mechanical interpretation of bonding in donor–acceptor complexes. The atomic virial theorem enables one to determine the contribution of each atom to the binding energy of the complex, as determined by the change in the atom's electronic kinetic energy. The theorem then enables one to relate this contribution to the changes in the atom's attractive and repulsive potential energies that result from the re-organisation of the density and accompanying interatomic charge transfers. The role of the KE in determining molecular stability has been extensively discussed [1,75,76]. The low values attained by the KE in particular spatial regions has been determined in conjunction with the virial theorem and without recourse to arbitrary reference states, using the positive definite form of the kinetic energy density $G(r) = (\hbar^2/2m)\langle\nabla\psi\cdot\nabla\psi\rangle$. It is shown that the pronounced local lowering of $G(r)$ in the binding region associated with bonding, $G(r) < \rho(r)$, is unique to hydrogen and that for atoms from the second row onwards, local decreases in $G(r)$ are found primarily in the antibinding regions.

6.2. Critique of energy partitioning methods

The published discussions of the bonding in donor–acceptor complexes contradict the unique stabilising role of the electrostatic attraction of the nuclei for the electron density. They employ the breakdown of the energies of interaction of the reactants into contributions from a series of imagined and physically unrealisable intermediate steps in energy decomposition analyses [30,77]. The steps are chosen so as to partition the energy of interaction into contributions the first of which, following on an initial promotion of the reactants if deemed necessary, is ascribed to electrostatic interactions followed by one ascribed to Pauli or exchange repulsions, and another to an 'orbital relaxation' contribution. Frenking et al. [25] choose to identify the electrostatic and orbital relaxation contributions with electrostatic (ionic) and covalent bonding respectively, claiming that these definitions as obtained from the energy partitioning scheme are a step towards 'a rigorously defined quantum chemical analysis of the chemical bond'.

Kunze and Davidson [33] applied the Morokuma energy decomposition analysis [77] to the bond energy in $Cr(CO)_6$, one that is summarised by Frenking and Frölich [24]. The model used to determine the 'electrostatic' contribution to the energy is obtained by placing the Cr atom, within a preassembled octahedral cage of the six ligands, with the bond length of each CO extended to its length in the complex, the Cr having been promoted in a previous step to the hypothetical $t_{1g}^6\,{}^1A_{1g}$ state, a state that is thought to best represent the atom within the complex. The 'electrostatic' contribution to the energy is determined by calculating the energy of this assembly with frozen electron density distributions, the resulting energy corresponding to one obtained from a wave function expressed as a simple product of the fragment functions thus violating the Pauli principle. This is followed by the calculation of the same system now described by a single Slater determinant, the orbitals on the fragments changing in response to the newly imposed orthogonality constraints acting on the two sets of fragment orbitals. The resulting exchange integrals lower the energy but this is overwhelmed by the 'repulsive terms due to the non-orthogonality of the orbitals'. This contribution is labelled the "exchange interaction" by Kunze and Davidson, and the exchange or Pauli repulsion by Frenking. In the final step, the 'relaxation energy' is obtained by allowing the orbitals in the Slater determinant obtained in the exchange interaction step to relax into their final forms in the complex.

Each of the above steps, as well as being physically unrealisable, leads to changes in the electron density and thus to changes in the electron–nuclear attractive interaction V_{en}, the sole source of energy lowering in complex formation. Frenking et al. [25] discuss the problems and artifacts associated with the partitioning scheme, particularly the inability to separate the 'electrostatic' from the 'covalent' or relaxation contributions. However, even the 'exchange interaction' leads to changes in the charge distribution and to changes in V_{en}. In particular, as detailed below, there are no 'Pauli repulsions', but rather charge redistributions leading to Feynman forces acting on the nuclei. The practitioners of the energy partitioning schemes justify the approach as a means of relating the results of quantum mechanical calculations to traditional bonding schemes and concepts. Kunze and Davidson [33], in their classical analysis of the bonding in $Cr(CO)_6$ conclude by asking the question: "Is it possible to extract from these pictures the 'driving force' for bond formation? For covalent bonds, the driving force is said to be the valence bond exchange effect from $\alpha\beta \leftrightarrow \beta\alpha$ 'spin-exchange resonance'. For ionic bonds, the driving force is ascribed to electron transfer at large R followed by Coulomb attraction between the ions. For hydrogen bonded complexes the driving force is electrostatic attraction between polar groups, and for non-polar van der Waals complexes it is induced-dipole-induced-dipole dispersion (another name for extra-molecular correlation energy)".

The following discussion demonstrates that the common "driving force" for all of the above bonding types is the lowering in energy caused by the new interactions of the nuclei in each reactant with the electron density in the product molecule. We follow Slater in making use of the virial and Hellmann–Feynman theorems to lay bare the physical origins of chemical bonding, theorems that Slater refers to as 'two of the most powerful theorems applicable to molecules and solids' [78]. The electron density that is necessarily accumulated in the binding region between a bonded pair of nuclei, as described by the 'exchange charge' of Heitler–London theory or the overlap density of molecular orbital theory, has two consequences: it lowers the potential energy, the magnitude of whose decrease is twice that of the increase in the kinetic energy, as required by the virial theorem, and because of this equality, the forces on the nuclei vanish, as demanded by Feynman's electrostatic theorem [1].

6.3. Electrostatic basis for homopolar and heteropolar bonding

We wish to establish that interactions classically labelled as ionic, polar, covalent, hydrogen bonded or van der Waals are equally the result of the accumulation of electron density between the nuclei with the above described consequences. Consider first the 14e molecules N_2 and CO and the 12e set, C_2 and LiF, molecules that provide examples of covalent, polar and ionic bonding. The atomic charges, bonding energies and the changes in V_{en}, V_{ee} and V_{nn} are given in Table 4. These results are from highly correlated QCISD calculations coupled with self-consistent virial scaling of the electronic coordinates (SCVS) employing a large basis set that give in excess of 90% of the experimental binding energies, the bracketed values under the heading D_e. The wave functions satisfy both the virial and Hellmann–Feynman theorems.

While the charge transfer in CO exceeds that in LiF, both the C and O atoms have significant residual valence density, density that is particularly evident in the large non-bonded charge distribution on C. It imparts to C a large 'back polarised' atomic dipole that results in a near vanishing molecular dipole moment. Thus, the charge distributions of neither C nor O approach their 'ionic' limit, as do the atomic distributions in LiF with atomic charges close to $\pm$1e [79]. The RHF delocalization indices are reported for the purpose of relating to the Lewis model [67]. One finds that of the 14 electrons in N_2, 3.0 are exchanged between the N atoms, corresponding to the sharing of three Lewis pairs. In CO on the other hand, only 1.6 electrons are exchanged between the atoms and as anticipated, the exchange of electrons between the atomic basins is less in the polar than in the homopolar interaction. Similarly in C_2, 2.7 of the 12 electrons are exchanged between the atoms while in LiF, where the atomic distributions approach their ionic form, only 0.18 are exchanged. The remaining electrons in LiF are localised within the atomic basins to

Table 4
Bonding energies and their potential contributions in AB[a]

AB	D_e	ΔV_{en}	ΔV_{en}^{o}	ΔV_{en}^{e}	ΔV_{ee}	V_{nn}	q(A)	R_e
N_2	9.13 (9.89)	−46.991	−2.639	−44.352	22.640	23.680	0.000	2.070 (2.074)
CO	10.8 (11.18)	−45.024	−2.996	−42.028	21.693	22.542	1.223	2.129 (2.138)
C_2	5.49 (6.0)	−30.616	−1.691	−28.925	14.920	15.292	0.000	2.354 (2.348)
LiF	6.22 (6.3)	−20.546	−4.280	−16.265	10.980	9.108	0.929	2.964 (2.960)

AB	ΔE(A)	ΔE(B)	ΔV_{en}(A)	ΔV_{en}^{o}(A)	ΔV_{en}^{e}(A)	ΔV_r(A)	ΔV_{en}(B)	ΔV_{en}^{o}(B)	ΔV_{en}^{e}(B)	ΔV_r(B)
N_2	−4.56	−4.56	−23.496	−1.320	−22.177	23.161				
CO	20.2	−31.0	−11.095	4.232	−15.327	12.582	−33.929	−7.228	−26.701	31.653
C_2	−2.75	−2.75	−15.309	−0.846	−14.463	15.107				
LiF	2.18	−8.39	−5.447	0.812	−6.259	5.607	−15.105	−5.092	−10.013	14.488

[a] QCISD/SCVS/6-311++G(2df), q(A) in units of e; D_e and $\Delta E(\Omega)$ in eV (exp); R_e and ΔV values in atomic units.

yield percent localisations of 96% for Li and 99% for F. The exchange indices clearly distinguish between ionic, polar and homopolar bonding, the ionic limit being characterised by an almost total localisation of the electrons within the basins of the atoms with a minimal exchange of electrons between them.

The decrease in the value of V_{en} from the separated atom values – its contribution to the bonding – is ∼2 au larger for homopolar N_2 than for polar CO, Table 4. The difference in the decreases in V_{en} is still greater for the 12e pair C_2 and LiF, with $|\Delta V_{en}|$ being ∼10 au larger for C_2 than for LiF. Thus, not only is the decrease in V_{en}, the electrostatic attraction of the nuclei for the density the source of the binding in both the homopolar and heteropolar molecules, it is of larger magnitude for the former than for the latter. The electron–nuclear potential energy for atom A, the quantity $V_{en}(A)$, is given by the sum of two contributions: the term $V^{o}_{en}(A)$, the interaction of the electron density in the basin of atom A (the density internal to A) with its own nucleus together with the term $V^{e}_{en}(A)$, the interaction of the same density with all the nuclei external to A. $V^{e}_{en}(A)$ *yields the stabilising interaction of the density of atom A with the nuclei of all the atoms that, together with A,are brought together in the formation of the molecule*. Thus, $V^{e}_{en}(A)$, which is zero for an isolated atom, is necessarily negative and it is the contributions of all the atoms to the decrease in V^{e}_{en} for the molecule that dominates the energy of formation.

This is made clear by the data in Table 4 giving the external, ΔV^{e}_{en} and internal, ΔV^{o}_{en} contributions from both atoms to ΔV_{en}. In all four molecules, the magnitude of ΔV^{e}_{en} far exceeds that of ΔV^{o}_{en} and the bonding in both sets of molecules is dominated by the electrostatic interaction of each nucleus with the density of the atom to which it is bonded. One also notes that ΔV^{e}_{en} is more negative for N_2 than for the polar molecule CO by 2.4 au, while the changes to the internal contribution, ΔV^{o}_{en}, differ by the lesser amount of 0.4 au. The same trend is found for the 12e molecules, with the magnitude of the external contribution for C_2 exceeding that for LiF by ∼13 au while the internal contributions equal –1.7 au for C_2 and –4.3 au for LiF. Thus, ΔV^{e}_{en} is the major contributor to the bonding in all four molecules and is of greatest magnitude for the homopolar molecules. What distinguishes the bonding within each set is not its physical origin, which in each case is a result of the decrease in V_{en}, primarily in the new attraction of each nucleus for the density of its bonded neighbour, but rather the manner in which the density is distributed over the two atomic basins and within the binding regions.

The atomic statement of the virial theorem determines the contribution of each atom to the bonding energy – the quantities of chemical interest – and relates these to the changes in the potential energy contributions. Each contribution arises from the change in the electron density over an atomic basin, a well-defined region of space. This enables one to identify the spatial origins of the energy change, with the energy of the atom changing by a little or by a lot as determined by the corresponding changes in its density, an obvious necessity of a physical theory.

For a system in an equilibrium geometry, the molecular virial equals the electronic potential energy V. It is useful to combine the two repulsive contributions to V into a single term $V_r = V_{ee} + V_{nn}$. This enables one to express $V(A)$, the atomic contribution to V, as the resultant of the attractive and repulsive contributions and relate them to the atom's electronic kinetic energy $T(A)$,

$$V(A) = V_{en}(A) + V_r(A) = -2T(A) \tag{7}$$

One has, in addition, further virial relationships relating $T(A)$ and $V(A)$ to the energy of atom A,

$$E(A) = -T(A) = \tfrac{1}{2}V(A) \tag{8}$$

Thus, the change in the atom's electronic kinetic energy determines the changes in its total energy and in its potential energy contributions given in Table 4,

$$\Delta T(A) = -\Delta E(A) = -\tfrac{1}{2}(\Delta V_{en}(A) + \Delta V_r(A)) \tag{9}$$

The dissociation energy $D_e = -(\Delta E(A) + \Delta E(B))$. The changes in the atomic energies are necessarily equal in the homopolar cases, but in the heteropolar molecules, they are positive for the electropositive atoms C and Li and negative for the electronegative partners, O and F, the recipients of charge transfer. The total repulsive contribution $\Delta V_r(A)$ exceeds the decrease in $\Delta V_{en}(A)$ for C and Li. This result is made understandable in terms of the atomic contributions to ΔV_{ne} which reflect the transfer of 1.2e from C to O and of 0.93e from Li to F, Table 4. The bonding is dominated by the decrease in $\Delta V_{en}(A)$ for the O and F atoms. In CO, the magnitude of $|\Delta V_{en}(O)|$ is ∼23 au greater than $|\Delta V_{en}(C)|$ while in LiF, $|\Delta V_{en}(F)|$ is ∼10 au greater than $|\Delta V_{en}(Li)|$. The charge transfer contributes to these disparities by causing the internal contributions to ΔV_{en} for both C and Li to increase, with $\Delta V^{o}_{en}(C) = +4.2$ and $\Delta V^{o}_{ne}(Li) = +0.8$ au, while the corresponding contributions for the O and F atoms decrease in value, with $\Delta V^{o}_{en}(O) = -7.2$ au and $\Delta V^{o}_{en}(F) = -5.1$ au. The atomic energy changes, like those for the molecule, are dominated by the external contributions to ΔV_{en} with the dominant contribution coming from the most electronegative atom. The interaction energy of the O nucleus with the atomic density on C, the quantity $\Delta V^{e}_{en}(C)$ equals −15 au, while the interaction of the C nucleus with the atomic density on O, the quantity $\Delta V^{e}_{en}(O)$, equals −27 au. The corresponding values of $\Delta V^{e}_{en}(Li)$ and $\Delta V^{e}_{en}(F)$ are –6 au and –10 au, respectively.

Thus, the *bonding* in all four molecules is a result of the accumulation of electron density in the bonding region, resulting in a decrease in V_{en}, a decrease that is primarily a result of the interaction of the density of one atom with the nucleus of its bonded partner. In polar and ionic molecules, the bonding is a result of the density accumulated in the basin of the most electronegative atom whose density is polarised towards the positively charged neighbour, a feature clearly reflected in the molecular charge distribution and the atomic dipolar

moments. The changing nature of the molecular charge distributions accompanying the formation of these molecules has been previously given [80]. Of particular interest is the abrupt transfer of charge from Li to F, beginning around 12 au and completed by 10 au, a result in accord with the 'harpoon mechanism' postulated for this reaction. The transfer of density from hydrogen to the base atom that occurs in hydrogen bonding similarly results in the destabilisation of the hydrogen and in a stabilisation of the base atom [81].

The *binding*, as determined by the *forces* exerted on the nuclei is, as pointed out by Berlin, a consequence of an excess of density being accumulated in the binding region between the nuclei, as opposed to its accumulation in the antibinding regions [82]. Thus, in homopolar molecules, the decrease in energy responsible for bonding and the net binding force on each nucleus is a consequence of the density accumulated in the internuclear region and shared equally by both atoms while in heteropolar systems, the bonding and binding are consequences of the density accumulated in the binding region of the most electronegative atom [1,83,84].

6.4. Electrostatic basis for van der Walls bonding

The accumulation of density between the nuclei and the resulting dominant decrease in V_{en} is also responsible for van der Walls bonding, as first pointed out by Feynman in his 1939 paper, which introduced the electrostatic force theorem: the force acting on a nucleus is the resultant of the electrostatic forces of repulsion exerted by the other nuclei and of attraction exerted by the electron density [85]. Feynman notes that the interpretation of the long-range R^{-7} force of attraction between neutral molecules in terms of 'induced oscillating atomic dipoles' would in fact lead to repulsive forces on the nuclei. This 'classical' interpretation is an attempt to recast the second-order perturbation description of the interaction that describes the correlation-induced changes in the *six-dimensional space* of the pair density in terms of classical-like dipoles in *real space*. The actual response of the distribution of electronic charge in real space to the correlative interactions is for the density of each atom to be polarized in the direction of the other, as pictured in the density difference map shown in Fig. 5 for the approach of two hydrogen atoms at a separation of 8 au obtained from a highly correlated wave function [86]. The inwardly directed atomic polarisations lead to an accumulation of density in the binding region, to a force of attraction on the nuclei and eventually to a lowering of the potential energy. Thus, the mechanism of bonding is no different from that for any bound state. The use of a correlated wave function for the description of molecule formation over the complete range of internuclear distances, as opposed to the use of specific theoretical models to treat different stages of the interaction, removes any bias for ascribing a special basis to van der Waals bonding. Such an approach has been illustrated for H_2, LiF, N_2, CO and Ar_2, all of which display the behaviour noted above for H_2 for large internuclear separations [80].The mechanics of the long-range

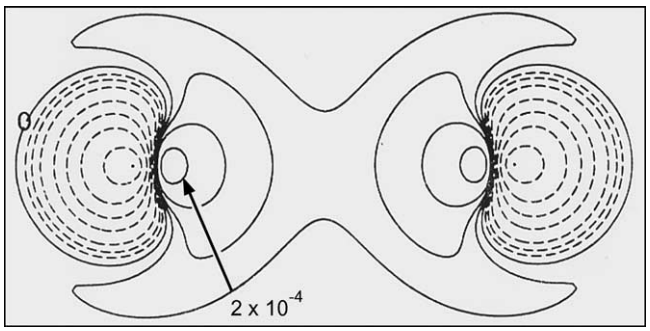

Fig. 5. Density difference map for H_2 with respect to separated ^{2}S H atoms at a separation of 8 au where the overlap of the atomic densities is negligible. The map illustrates the polarisation of each atomic density caused by the correlative interaction of the two electrons. The decrease in the density in the region of each nucleus causes the potential energy to increase and the kinetic energy to decrease. Its accumulation in the binding region results in a 'van der Waals force' of attraction, a Feynman force on the nuclei. The solid and dashed contours increase (+) or decrease (−) from the zero contour in steps $\pm 2 \times 10^n$, $\pm 4 \times 10^n$, $\pm 8 \times 10^n$ au with n beginning at −5 and increasing in steps of unity.

attractive interactions between the atoms encountered in the initial stages in the formation of these molecules deserves further comment. The relevant statement of the virial theorem relating $\Delta T(R)$, the change in the kinetic energy to $\Delta E(R)$ at a separation R, referenced to the separated atom values, is given in Eq. (10)

$$\Delta T(R) = -\Delta E(R) - R\frac{\mathrm{d}E}{\mathrm{d}R} \tag{10}$$

The term $R(\mathrm{d}E/\mathrm{d}R)$ is the virial of the Feynman force $F(R) = -(\mathrm{d}E/\mathrm{d}R)$, exerted on the nuclei. Only when the forces on the nuclei vanish does one obtain the result $\Delta T(R) = -\Delta E(R)$, that the magnitude of the decrease in energy equals the increase in the kinetic energy. The virial and Feynman theorems may be combined by differentiation of Eq. (10) to yield constraints on the values of $\mathrm{d}T/\mathrm{d}R$ and $\mathrm{d}V/\mathrm{d}R$ as a function of R [1,76]. Because of the creation of an attractive force for large R, the virial theorem requires the kinetic energy to initially decrease and the potential energy to increase, just the opposite behaviour to that found at the equilibrium separation. The virial of the attractive force is stabilising and consequently, the initial decrease in ΔT is of smaller magnitude than the decrease in E. As one approaches the equilibrium separation, T begins to increase and V to decrease and at $R = R_e$, one recovers the result that the binding arises from a decrease in V, with $\Delta E = (1/2)\Delta V = -\Delta T$. The virial of the nuclear force makes a repulsive contribution to the energy for separations $R < R_e$, the repulsive region of the potential curve and ΔT then exceeds $|\Delta E|$. For example, the approach of two He atoms to a separation 1.9 au for which $\Delta E = +96$ kcal/mol, results from $\Delta T = +286$ kcal/mol and $\Delta V = -190$ kcal/mol, and T exceeds the magnitude of E by the virial of the repulsive nuclear force, $\mathrm{RF}(R) = 382$ kcal/mol.

The initial decrease in T and increase in V caused by the charge reorganisation associated with the creation of the attractive force is made clear in Fig. 5. Density is removed

from each of the antibinding regions, up to and including the nucleus where the local potential energy is maximally stabilising, leading to the increase in V. The steep gradients in the wave function and density in the region of a nucleus make large local contributions to the kinetic energy and the removal of density from the vicinity of each nucleus leads to the decrease in T. Density is accumulated in the form of a diffuse distribution in the binding region between the nuclei where it exerts attractive forces on both nuclei. This explanation exemplifies the physical understanding afforded by a theory couched in terms of the changes incurred in a molecular charge distribution and their interpretation in terms of the accompanying changes in force and energy, as governed by the virial and Feynman force theorems.

It is well documented that the differences in the distribution of density within the binding regions of shared, polar and closed-shell interactions are succinctly summarised in the topological and energy parameters at the bond critical point. The local expression of the virial theorem relates the potential and kinetic energy densities to $\nabla^2\rho_b$, the Laplacian of the density at the CP. The changes in the energy and the charge distributions over the entire range of internuclear separations for H_2, N_2, CO, Ar_2 and LiF have been previously given to illustrate the interplay between the changes in the kinetic and potential energies on bond formation [80].

6.5. Electron exchange, 'resonance' and 'Pauli repulsions'

It is necessary to establish how the changes in the electrostatic contributions to the energy as enshrined in the Hamiltonian, are tempered by the requirements of the Pauli principle. These requirements are described neither by 'resonance' nor by 'Pauli repulsions', but are instead determined through the mechanism of electron exchange, the consequence of incorporating the requirement of antisymmetry into the wave function. Quantum mechanical exchange, defined by the exchange operator, plays a unique and important role in chemistry [59]. The role of this operator and the phenomenon of exchange can be determined directly rather than being disguised in non-physical terms such as 'resonance', 'Pauli or exchange repulsions' and 'covalency'.

Slater pointed out that the exchange term of Hartree–Fock theory can be rewritten in terms of an 'exchange charge density' the name he applied to what is now commonly referred to as the density of the Fermi hole [87,88]. Section 5 demonstrates how this density may be incorporated into the mechanics of bonding through the definition of the exchange indices. The statement of Kunze and Davidson [33] that the driving force for covalent bonds "is said to be the valence bond exchange effect from $\alpha\beta \leftrightarrow \beta\alpha$ 'spin-exchange resonance"' leads one directly to the delocalization index δ(A, B). This index provides a quantitative measure of 'spin-exchange resonance' by determining the number of $\alpha\beta$ electron pairs participating in the exchange between the atoms A and B. The role of exchange in determining the energy is to reduce the electron–electron Coulomb repulsion between a pair of bonded atoms, and δ(A, B) counts the number of electrons contributing to this reduction. The weighting of the exchange operator with $1/r_{12}$ in the integration over the atomic basins yields the decrease in energy resulting from the exchange between a given pair of atoms, the essence of the 'resonance contribution' to bonding. Pendás et al. [89] have recently programmed two-electron integrations over atomic basins enabling the calculation of the exchange energy determined by the delocalisation index, resulting in the 'resonance energy of interaction' and obviating the need to invoke the resonance structures of valence bond theory. Professor Pendas has kindly supplied us with the values of the inter-basin exchange energies at the RHF level for the 14- and 12-electron series discussed in Section 6.3. As anticipated, they parallel the relative values of the corresponding delocalisation indices. The values of the inter-basin exchange energies in all are -0.951 for V_{ex}(N, N) and -0.442 for V_{ex}(C,O) giving a ratio of 2.2 compared to the ratio δ(N,N)/δ(C,O) = 1.9. The corresponding values for the 12-electron series are -0.717 for V_{ex}(C,C) and -0.045 for V_{ex}(Li, F) giving a ratio of 16 compared to the ratio δ(C,C)/δ(Li,F) = 15. The contribution of '$\alpha\beta$ Spin-exchange resonance' clearly decreases with increasing polarity of the interaction, its value in ionic LiF accounting for only 0.4% of the total exchange energy.

Within the orbital model, imposition of the Pauli principle is equivalent to requiring the orbitals to be orthogonal. The translation of this mathematical constraint into a physical picture has been investigated by imposing the orthogonality constraint on the density distribution of an initially assigned set of fragment orbitals [90]. In the minimal case of two normalised doubly occupied atomic orbitals ϕ_a and ϕ_b with overlap S, the density in the absence of the orthogonality constraint is given by $\rho = 2(\phi_a^2 + \phi_b^2)$ while its imposition causes a change in the density $\Delta\rho$ that is given by

$$\Delta\rho = -4S\phi_a\phi_b + 2S^2(\phi_a^2 + \phi_b^2) \tag{11}$$

a term that integrates to zero and is correct to second-order in S [91]. The form of $\Delta\rho$, as shown in Fig. 6, is exceedingly simple: it removes density from the region of overlap between the two centres a and b, the binding region, and accumulates it in the antibinding regions [82], (regions whose boundaries are indicated in the figure) a change in density that results in electrostatic forces of repulsion acting on the nuclei. It is the opposite of the corresponding diagram in Fig. 5 responsible for the long-range attractive forces. Thus, the effect of antisymmetrization is to remove density from the region of overlap of the occupied orbitals and to create a force of repulsion on the nuclei. The 'Pauli force' is in fact the Feynman electrostatic repulsive force acting on the nuclei. The Feynman force determines the gradients of the potential energy surface and the resulting increase in energy for the approach of two closed-shell systems is obtained by integrating the repulsive Feynman force on the nuclei over the decrease in their internuclear separation.

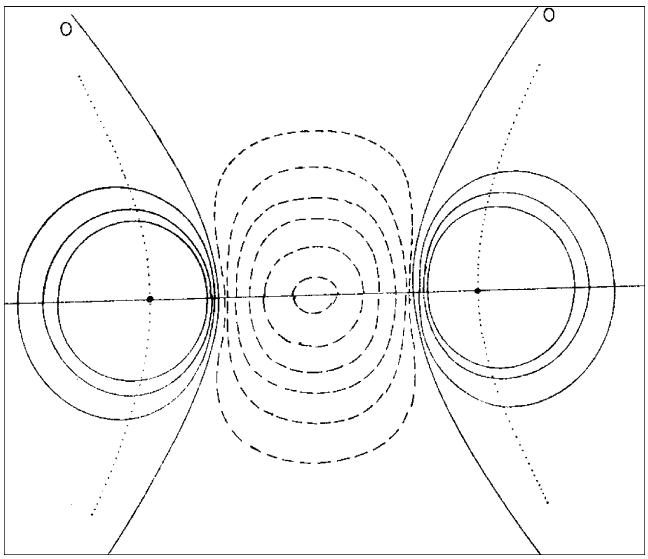

Fig. 6. A contour display of $\Delta\rho$, Eq. (11), applied to two He atoms at a separation of 2.5 atomic units. The dotted lines that pass through the nuclei are the boundaries separating the binding from the two antibinding regions. The contour values increase (solid) or decrease (dashed) in steps of 0.002 au from the zero line.

The presence of 'Pauli repulsions' between atoms are frequently invoked without a physical basis to account for geometries or for the origin of barriers, particularly between hydrogen atoms: between the *ortho*-hydrogens in the rotation of biphenyl into a planar geometry; between the hydrogens of *tert*-butyl groups used to corset unstable molecules; between a hydrogen of a *tert*-butyl group and the 1,3 diaxial hydrogens in substituted cyclohexanes and in the eclipsed form of ethane. In none of these cases do forces act on the protons in the final geometry, nor is the geometry the result of the action of repulsive forces acting on the protons [56,92,93].

While the picture of $\Delta\rho$ for the example of two orbitals coincides with the common picture of 'colliding orbitals', its form for systems with more than two occupied orbitals no longer corresponds to this interpretation. With N electrons, there are $N/2$ occupied orbitals (N assumed even) and the orthogonality restraint is imposed not in three-dimensional space physical space, but in the $N/2$ mathematical space and the resulting display of $\Delta\rho$ bears no simple relationship to the physical picture of 'colliding orbitals [90]'.

It is not clear what useful information is obtained in the 'Pauli repulsion' step of the energy partitioning procedure, since the lowest energy pathway will, where possible, correspond to one in which the atoms are oriented so as overlap favourably with one another. Consider an energy partitioning analysis for the formation of CO. Both atoms are non-spherical, having ^{3}P ground states and one must choose which states of the atoms are to be employed in the product of the overlapping atomic wave functions that is to be eventually antisymmetrised. The correct 'valence states' *are* determined in a quantum mechanical calculation of the initial approach of the atoms, the density of both atoms being ellipsoidal, with the major axis for C being perpendicular to the internuclear axis, that for O being coincident with it. The associated Laplacian distribution, as previously demonstrated, accounts for this orientation by showing that it places a 'hole' in the valence shell charge concentration of C in line with the local charge concentration on O [80]. This is the opposite to the picture of 'Pauli repulsions' between filled pairs of orbitals that are pictured to occur when overlapped atomic wave functions are antisymmetrised, whatever atomic states are arbitrarily chosen. There are of course repulsions between the electrons on the two atoms but orbital orthogonality is maintained at all times and the energy undergoes a smooth and continuous decrease as each nucleus interacts with the density of the approaching atom. The delocalization of the exchange density between the two atomic basins undergoes a continuous increase with decreasing R, indicating the overriding importance of the filling of orbital vacancies on the two atoms and of a favourable exchange interaction. The Laplacian distribution shows a smooth filling of both the bonded and non-bonded holes on C with the resulting formation of a bonded concentration of charge between the nuclei and of a non-bonded charge concentration (CC) on each atom [80]. The non-bonded CC on C is particularly pronounced and is responsible for its exceptional donor ability, as exemplified below.

7. Energy contributions to bonding in complex formation

7.1. Changes in the attractive and repulsive potential energies

The changes in the attractive, ΔV_{en}, and repulsive, ΔV_{ee} and ΔV_{nn}, contributions to the energy of formation ΔE of the carbonyl complexes and ferrocene are given in Table 5. The total change in the repulsive contribution $\Delta V_r = \Delta V_{ee} + \Delta V_{nn}$ is also listed. The changes ΔV_{en} and ΔV_r, reported in atomic units (au), are of extremely large magnitude compared to their sum that, by the virial theorem, yields twice the total change in energy, the binding energy ΔE, Eq. (8). The change in the attractive contribution, ΔV_{en}, is necessarily negative, its magnitude decreasing in the order Cr, Fe, Ni, an order that parallels the decreasing number of ligand atoms. It is well to appreciate the magnitudes of the forces involved in the formation of these complexes and of molecules in general, and of the need for a means of isolating the changes that are

Table 5
Bonding energies and their potential contributions in complexes[a]

Complex	ΔE	ΔV_{en}	ΔV_r	ΔV_{ee}	ΔV_{nn}
$Cr(CO)_6$	−155	−1681.699	1681.205	838.538	842.667
$Fe(CO)_5$	−166	−1370.253	1369.723	682.837	686.886
$Ni(CO)_4$	−123	−1011.846	1011.452	504.345	507.108
$Fe(Cp)_2$	−170	−1222.210	1221.667	610.218	611.449

[a] ΔE in kcal/mol, ΔV in atomic units.

Table 6
Atomic charges and changes in population for complex formation

Complex	q(M)		q(C)	q(O or H)	ΔN(M)	ΔN(C)	ΔN(O or H)
$Cr(CO)_6$	1.16		0.93	−1.12	−1.16	0.22	−0.03
$Fe(CO)_5$	0.74	ax	1.00	−1.11	−0.74	0.15	−0.04
		eq	0.95	−1.12		0.20	−0.03
$Ni(CO)_4$	0.51		1.00	−1.12	−0.51	0.15	−0.02
$Fe(Cp)_2$	0.79		−0.16	0.08	−0.79	0.08	0.00
$Al(Cp)_2^+$	2.35		−0.28	0.14	−1.35	0.19	−0.06
$Ge(Cp)_2$	0.86		−0.10	0.02	−0.86	0.02	0.06

CO: q(C) = 1.150, q(O) = −1.150; $Cp^•$: q(C) = −0.084, q(H) = 0.080; Cp^-: q(C) = −0.184, q(H) = −0.016.

of chemical interest, a need that, as described above, is met by the atomic statement of the virial theorem.

7.2. Atomic charges

The atomic charges and changes in atomic populations, Table 6, summarise the principal redistributions of charge accompanying the formation of the complexes. Frenking and Frölich state "atomic partial charges are not an observable (measurable) quantity" [24] and proffer this as an apology for the many definitions found in the literature and the necessity of using personal preferences in choosing between them. While this statement most certainly applies to the definitions expressed in terms of the orbital model, such as natural bond orbitals [94] and charge decomposition (CDA) [95] analyses, it does *not* apply to the population of an open quantum system [79]. *An atomic population as defined within QTAIM is the expectation value of a Dirac observable* [96] *and is now routinely measured in accurate X-ray diffraction experiments on crystals*.

The major transfer of electron density in the formation of a metal carbonyl is from the metal atom to the carbon atoms of the ligands. The amount transferred is not large, with the charge transfer per CO ligand equalling 0.19, 0.15 and 0.13e, respectively for Cr, Fe and Ni. The charges on the metal atoms are in close agreement with those of Macchi and Sironi [31], differing at the most by 0.05e. The increases in the populations of carbon range from 0.22e for the Cr complex to 0.15e for the Ni complex. There is a small accompanying transfer of density from oxygen to carbon, in amounts ranging from 0.02 to 0.04e within each CO group.

The major transfer of density in the metallocenes is from the metal to the carbons of the Cp rings. The changes in the C and H populations for the Cp rings are given with respect to the average of the atomic values in the Cp radical. The charge of 0.79e transferred from Fe to the ligands in ferrocene is the same to within 0.05e of the amount transferred in its pentacarbonyl complex, the charge being transferred solely to the carbons of the ligands in both molecules.

7.3. Atomic contributions to bonding energy in carbonyl complexes

The principal atomic contribution to ΔE in the formation of the donor–acceptor complexes is from the metal atom, the values ΔE(M) in Table 7. The stabilising decrease in the attractive potential energy ΔV_{en}(M) is of large magnitude and arises entirely from the decrease in the external contribution, V_{en}^{e}(M). This contribution, the attraction of the density of the metal atom M with all the nuclei *external* to the basin of M, is dominant in the formation of the complex. It yields the stabilizing interaction of M with the nuclei of all the atoms that, together with M, are brought together in the formation of the complex. The internal contribution for the metal atoms, ΔV_{en}^{o}(M), is positive and orders of magnitude smaller, being a result of the transfer of charge from the metal to the carbon atoms of the ligands. In general, a (stabilising) decrease or (destabilising) increase in the value of the internal contribution V_{en}^{o}(A) relative to its free atom value is determined by a corresponding increase or decrease in the electron population of A, the quantity ΔN(A), Table 6. Thus, ΔV_{en}^{o}(A) is positive for the metal atoms and for the oxygen atoms and negative and stabilising for the carbon atoms because of the transfer of electron density to carbon

Table 7
Atomic contribution to bonding energies and their potential contributions[a]

Complex	ΔE(M)	ΔV_{en}(M)	ΔV_{en}^{e}(M)	ΔV_{en}^{o}(M)	ΔV_r(M)
$Cr(CO)_6$	−620	−406.468	−414.766	8.299	404.491
$Fe(CO)_5$	−720	−395.077	−399.472	4.395	392.782
$Ni(CO)_4$	−675	−341.723	−344.605	2.882	339.571
$Fe(Cp)_2$	−645	−426.294	−430.777	4.483	424.516
	ΔE(C)	ΔV_{en}(C)	ΔV_{en}^{e}(C)	ΔV_{en}^{o}(C)	ΔV_r(C)
$Cr(CO)_6$	−59.7	−94.760	−93.780	−0.980	94.570
$Fe(CO)_5$					
ax	−47.8	−88.114	−87.306	−0.808	87.962
eq	−42.2	−88.113	−87.231	−0.882	87.978
$Ni(CO)_4$	−16.0	−76.336	−75.690	−0.647	76.285
$Fe(Cp)_2$	46.7	−71.126	−70.984	−0.142	71.275
	ΔE(O)	ΔV_{en}(O)	ΔV_{en}^{e}(O)	ΔV_{en}^{o}(O)	ΔV_r(O)
$Cr(CO)_6$	137	−117.837	−118.176	0.339	118.275
$Fe(CO)_5$					
ax	155	−106.515	−106.890	0.375	107.010
eq	156	−107.579	−107.988	0.409	108.075
$Ni(CO)_4$	154	−91.174	−91.545	0.371	91.666
$Fe(Cp)_2$ (H)	1.14	−8.291	−8.294	0.003	8.295

[a] ΔE in kcal/mol, ΔV in atomic units.

from the metal atom and to a lesser extent, from the oxygen atoms.

The contributions for $Cr(CO)_6$ are used to exemplify the atomic contributions to ΔE. The 8 kcal/mol error in the calculated binding energy, or 2 kcal/mol per ligand, is too small to affect the discussion. The binding energy of 156 kcal/mol arises from a decrease of 620 kcal/mol in the energy of the Cr atom that is accompanied by a decrease of 60 kcal/mol in the energy of each carbon of CO. These stabilising energy changes are partially offset by an increase in the energy of each oxygen of CO by 137 kcal/mol, Table 7. Thus, the binding in the metal carbonyls is a result of two contributions: (1) the dominant and exceptional decrease in the energy of interaction of the density on M, shown in Fig. 1 for the Cr atom, with the nuclei of the surrounding cage of ligand atoms, the term $\Delta V_{en}^{e}(M)$: (2) the stabilisation of the carbon atoms resulting from the transfer of density to carbon primarily from the metal atom, the transferred density causing both $\Delta V_{en}^{o}(C)$ and $\Delta V_{en}^{e}(C)$ to decrease and contribute to the stabilisation. It is demonstrated below that the electronic charge transferred to carbon is distributed in the form of a π-like torus of density encircling the C–O axis, in the manner envisaged in the Dewar–Chatt–Duncanson model of dπ–pπ* back bonding [97,98].

The net destabilisation of the CO ligands is a result of the charge transfer from oxygen to carbon. The changes in the attractive and repulsive contributions that result from the placement of the CO ligand in the complex, the quantities ΔV_{en}^{e} and ΔV_r, are nearly balanced for both C and O, with the external contribution to the potential energy decrease being of slightly smaller magnitude than the increase in the repulsive contribution in all three complexes. However, because of the charge transfer from both M and O to C, the change in the internal contribution V_{en}^{o}, while small in magnitude, is stabilising for carbon and destabilising for oxygen and it is this contribution that tips the balance between the overall energy change being stabilising for C and destabilising for O. The decrease in the magnitude of $\Delta V_{en}^{o}(C)$ parallels the decrease in the charge transferred to carbon, the order Cr > Fe_{eq} > Fe_{ax} ∼ Ni. The decrease in $V_{en}(C)$ is same to within 1 kcal/mol for C_{ax} and C_{eq} in $Fe(CO)_5$, but $\Delta V_r(C_{eq}) > \Delta V_r(C_{ax})$ by 5 kcal/mol and hence C_{ax} is more stable than C_{eq}. The Laplacian distribution for $Fe(CO)_5$ reported below, shows that the axial CO ligands are directed at holes in atomic graph of Fe, while the equatorial ligands are directed at secondary maxima, the (3, −1) cps in edges of atomic graph, thereby accounting for the increased contribution to the energy of repulsion in the latter over the former ligands.

7.4. Atomic quadrupole moment as a measure of dπ–pπ* back-bonding

In the Dewar–Chatt–Duncanson (D–C–D) dπ–pπ* model of back-bonding, the t_{2g} electrons of the metal are delocalized into the antibonding π* orbitals of the ligands [97,98]. There is no agreement on the importance of this back-bonding in the formation of the carbonyl complexes when interpreted using the orbital model or any of the energy decomposition schemes. Kunze and Davidson [33], for example, state that their conclusion that 3d–2π* covalent mixing is not the primary source of bonding in $Cr(CO)_6$ is one "with which many people can reasonably disagree" as would Bauschlicher and Bagus [99] who state "It is now generally agreed that the back-bonding is dominant and that the σ donation is mainly to the $3de_g$ orbital". If indeed operative, the D–C–D model will have consequences on the properties of the charge distributions and energies of the metal and their bonded carbon atoms that may be determined using QTAIM.

The most immediate effect would be to change the quadrupole moment of the CO ligands upon bonding in the complex. The quadrupole moment of an axial molecule provides a determination of the accumulation of σ-like electron density along the molecular axis, as opposed to its π-like accumulation in a torus about the axis. The atomic quadrupole moment is defined as a traceless tensor and thus the component parallel to the axis $Q_{\parallel}(A)$, and its two perpendicular components $Q_{\perp}(A)$, sum to zero. Because of this, the changes in the parallel or perpendicular components provide a direct determination of the extent of transfer of density between the σ and π systems of a linear molecule. The magnitude $|Q(A)|$ of the atomic quadrupole polarisation and the perpendicular component, $Q_{\perp}(A)$, are given in Table 8 for isolated and bound CO groups. The value of the axial component $Q_{\parallel}(A) = -2Q_{\perp}(A)$. The valence density of the carbon atom in a free CO molecule exhibits a very pronounced polarisation into its non-bonded region, an effect strikingly evident in its Laplacian map discussed below, and responsible for the vanishingly small dipole moment of CO [79]. Thus, the axial component nearly cancels the perpendicular component arising from the π density and $|Q(C)|$ is relatively small.

The increases in the magnitude of the quadrupole moment of a carbon and its perpendicular contributions are dramatic when the CO molecule is complexed. $|Q_{\perp}(C)|$ increases by a factor of 8 for Cr and 10 for Ni. $|Q(C)|$ increases by factors ranging from 8 to 12, with the maximum occurring for the equatorial carbon in the iron complex and decreasing in the

Table 8
Atomic quadrupolar moments in carbonyl complexes in atomic units

Molecule	Ω		$Q_{\perp}(\Omega)$	$\lvert Q(\Omega)\rvert$
CO	C		−0.1067	0.2135
$Cr(CO)_6$			−0.8766	1.7532
$Fe(CO)_5$		ax	−0.9277	1.8553
		eq	−1.1685	2.4776
$Ni(CO)_4$			−1.1241	2.2476
CO	O		−0.1242	0.2485
$Cr(CO)_6$			−0.1727	0.3454
$Fe(CO)_5$		ax	−0.1662	0.3321
		eq	−0.1935	0.3872
$Ni(CO)_4$			−0.1671	0.3341

$|Q(\Omega)| = \sqrt{(2/3)[Q_{xx}^2 + Q_{yy}^2 + Q_{zz}^2]}$.

order Ni > Cr ∼ Fe for axial C. The quadrupole polarisation of carbon in the complex is dominated by the toroidal accumulation of density, a consequence of the increase in its π density distribution. Thus, Q(C) provides a quantifiable demonstration of the increase in π density, both absolutely and relative to the σ density of a carbon atom that accompanies its complexation. The effects are smaller by an order of magnitude for oxygen, with only a small increase in the magnitude of its perpendicular components.

Section 8 demonstrates how the atomic overlap matrix bridges molecular orbital models and the atomic properties of QTAIM. A diagonal element of this matrix yields the number of electrons of a given orbital that reside within an atomic basin, enabling the assignment of contributions from individual orbitals to an atomic population. The orbital contributions clearly indicate the importance of dπ–pπ* backbonding from M to the carbons of the ligands, relative to σ donation from the ligands to the metal. Of the 12 electrons in the t_{1u}, e_g and a_{1g} sigma bonding orbitals in $Cr(CO)_6$, only 0.95e reside on the metal atom, while of the six electrons in the t_{2g} set, 3.6e remain on Cr while the remaining 2.4e reside on the ligands, with 0.25e on each carbon. By symmetry, these electrons occupy the 2π* antibonding orbital of CO. The association of the "a" and "e" orbitals of the axial ligands in $Fe(CO)_5$ with the respective σ and π orbitals of the ligands enables one to determine that the π population of an axial carbon atom increases by 0.32e on bonding to Fe, while its σ population undergoes a decrease of 0.22e.

7.5. Bonding in ferrocene

Table 5 gives the attractive and repulsive contributions to the energy changes in the formation of ferrocene from iron in its ^{5}D ground state and two neutral cyclopentadienyl radicals. The calculated value of ΔE of −170 kcal/mol is similar to the value of 166 kcal/mol obtained for $Fe(CO)_5$. Like the carbonyl complexes, the interatomic charge transfers and the charge transferred per ligand are small. The delocalisation indices δ(Fe, C) demonstrate the existence of a substantial exchange of electron density on Fe with the density on the carbon atoms of the Cp rings, the exchange of ∼4 electrons translating into the sharing of two Lewis pairs between the iron atom and each ring, as predicted by Moffit [58]. This, coupled with the bond CP properties, indicate that the Fe–C interactions, like the M–C interactions in the carbonyl complexes, are predominantly shared interactions.

The atomic contributions to ΔE are given in Table 7. The largest of these, and the single stabilising one, is from the Fe atom with ΔE(Fe) = −645 kcal/mol, the same magnitude as that for ΔE(M) in the carbonyl complexes. The decrease in ΔE(Fe) is a consequence of the external contribution to ΔV_{ne}(Fe), and the bonding in ferrocene is, like that in the carbonyl complexes, primarily a result of the stabilisation of the density on the metal atom by its interaction with the encompassing cage of carbon atoms.

Each Cp ring is destabilised by 239 kcal/mol on complexation. The rings are destabilised relative to their radical state in spite of the charge that is transferred to them from Fe, in the amount of 0.08e per carbon. The total charge on each Cp ring, equal to −0.40e, is intermediate between the charges of zero and minus one on the radical and anion while the C–C bond length in the complex, equal to 2.687 au, is longer than the average of the lengths in the radical, 2.674 au, and in the anion, 2.667 au. The delocalization of the density between neighbouring carbons and between next nearest neighbours equals 1.30 and 0.10, respectively, compared to the values in the anion of 1.39 and 0.13 that characterise 'aromatic' behaviour. Thus, the symmetrisation of a Cp ring on bonding to the iron atom results in a geometry, net charge and electron delocalization that fall short of the values found in the symmetrical anion with its particular $4n + 2$ stabilisation, and in addition result in the loss of the stabilising characteristics associated with the radical because of the overall increase in C–C separations.

The source of the bonding energy in $GeCp_2$, with ΔE = −129 kcal/mol, is similar in all respects to that in ferrocene. The Ge atom is stabilised by 703 kcal/mol and each Cp ring is destabilised by 287 kcal/mol, compared to corresponding values of −645 and +237 kcal/mol in ferrocene. The bonding energy in $AlCp_2^+$ however, is a result of the stabilisation of the Cp rings, each ring being stabilised by 60 kcal/mol with Al being stabilised by only 3 kcal/mol. This difference is understandable since, with a charge of +2.4e, Al has a valence population of only 0.6e and there is considerable charge transfer to the Cp rings, with each ring bearing a net charge of −0.70e, Table 6. In the Fe and Ge metallocenes, the charges on the metal atoms are less than unity. The atomic overlap matrix shows that Fe possesses 18.0 and Ge 28.0 localised core electrons and there is no significant exchange of the core electrons with the remainder of the molecule. Thus, Fe and Ge possess 7 and 3 valence electrons, respectively, and it is the valence density on the Fe and Ge metallocenes that is stabilised, while in the $AlCp_2^+$ it is the density on the Cp rings that is the source of the bonding. The delocalisation indices bear out this interpretation; the delocalisation between the metal and the rings is least for Al and the values of δ(C, C′) for the Cp rings, Table 2, because their charges of −0.7e, are nearly coincident with the value for the anion and its aromatic stabilisation.

8. Bridging MO theory and QTAIM

One may link molecular orbital models to the atomic properties of QTAIM by making use of the atomic overlap matrix whose elements S_{ij}(A) determine the overlap of orbitals i and j over the basin of a given atom A. A diagonal element S_{ii}(A) yields the number of electrons of orbital i that reside within the basin of atom A. The use of *individual* orbital contributions to any property, a step that involves the choice of a particular orbital representation, is arbitrary. The

use of orbital contributions is however, unavoidable if one wishes to bridge the MO interpretation of bonding in a metal complex with the atomic properties of QTAIM. The maximum correspondence with the standard orbital models and orbital correlation diagrams is obtained through the use of the Hartree–Fock (HF) canonical set which have been determined for the DFT optimised geometries. The procedure is less arbitrary if the contributions are grouped into symmetrically equivalent sets. The goal is to determine the contribution of the "d" orbitals to the atomic population of the metal and to gauge the relative importance of the charge transfers involved in ligand to metal and in the back-bonding from metal to ligand. In this manner, one may obtain answers to questions that are central to the orbital interpretation of bonding in a metal complex.

The contributions of the [Ar] core orbitals to the metal populations sum to 17.9e for Cr and 18.0 for Fe and Ni. The net charges on the metal atoms, from a maximum of +1.2e on Cr, would indicate that within the orbital model, each metal atom retains close to its d orbital population in the complex, assuming the density of the d orbitals to be contained within the zero-flux boundary of the metal atom. An upper bound to the d orbital population on M is obtained by assuming that the contributions from the orbitals of requisite 'd' symmetry are from its d orbitals.

8.1. $Cr(CO)_6$

The HF orbital configuration for the DFT optimised geometry of $Cr(CO)_6$ is $\ldots t_{1g}{}^6 e_g{}^4 t_{1u}{}^6 t_{2g}{}^6;\ {}^1A_{1g}$, in agreement with Kunze and Davidson [33]. Because of the molecule's O_h symmetry, the s, p and d orbitals of Cr belong to different irreducible representations with the metal d orbitals determining the e_g and t_{2g} contributions to the population on Cr, denoted by N(Cr). The e_g and t_{2g} contributions are 0.51 and 3.59e, respectively, for a total 'd' population of 4.1 in the complex, a number somewhat less than the free atom value of five in the ground configuration $[Ar]4s^1 3d^5$. The next most significant orbital contribution to N(Cr) is from the t_{1u} set that equals 0.29e. The t_{1u} and e_g orbitals, along with a_{1g}, which contributes 0.13e to N(Cr), are deemed responsible for the σ bonding with the CO ligands. Only 0.93e of the 12 electrons in these sigma bonding orbitals reside on the metal atom and it is clear that there is only a small amount of charge transfer from the 5σ orbital of CO onto the metal atom. The sum of these contributions, when added to the core population, accounts for all but 0.5e of N(Cr).

It is the upper t_{2g} set that participates in the D–C–D model of dπ–pπ* back-bonding and of the six electrons in this orbital, 2.4e reside on the ligands, 0.25e on each carbon and 0.15e on each oxygen. The t_{2g} contribution to N(Cr) of 3.6e accounts for all but ∼1.2of the Cr valence electrons. Ascribing these 1.2e to σ bonding indicates that the transfer of σ density from the ligands to the metal is only ∼50% as great as the transfer of density from the metal to π* orbitals of the ligands.

8.2. $Fe(CO)_5$

The HF electron configuration for $Fe(CO)_5$ is $\ldots e'^4 a''^2_2 a'^2_1 e''^4 e'^4;\ A'_1$. The d orbitals on Fe transform as do the top three orbitals, with the associations $e'(x^2–y^2, xy)$, $e''(xz, yz)$ and $a'_1(z^2)$, with the s and p orbitals on iron transforming as a'_1, e' and a''_2. The ground configuration of Fe is $[Ar]4s^2 3d^6$ and the Fe populations of the orbitals of d symmetry total 5.8e. This represents a loss 0.2e from the free atom value of six d electrons assuming that the a_1' and e' orbitals do not contain contributions from the metal 4s and 4p or ligands. The e'' orbitals overlap only with the π orbitals on the ligands while the e' orbitals can overlap with both σ and π on the equatorial ligands but only with π on the axial ligands. For the axial ligands, orbitals of "a" symmetry overlap only with σ orbitals on the ligands and those of "e" symmetry only with those of π symmetry. Thus, one may use the "a" and "e" orbital contributions to the axial C and O populations in $Fe(CO)_5$ to separately determine the number of electrons in the σ and π orbital sets on these two atoms in the complex and thus determine how they change from their values in unbound CO. This calculation shows that an axial carbon atom gains 0.32 π electrons and loses 0.22 σ electrons in forming the complex while the corresponding changes for the axial oxygen are much smaller, the atom gaining only 0.04e in π and losing 0.06e in σ. Thus, the increase of 0.1e in the HF population of a carbon atom in forming the iron complex is a result of an increase of 0.32e in its "e" or π set and a loss of 0.22e in the "a" or σ set. Clearly, the D–C–D model of dπ–pπ* backbonding is the dominant mode of electron transfer from the metal to the ligand in the formation of both $Cr(CO)_6$ and $Fe(CO)_5$.

8.3. $Ni(CO)_4$

The HF electron configuration of $Ni(CO)_4$ is $\ldots t_1^6 t_2^6 e^4 t_2^6;{}^1A_1$, an ordering identical to given by Miessler and Tarr [100] and to that obtained by Hillier and Saunders [101]. The contributions of these upper orbitals to N(Ni), beginning with t_1, are 0.00, 1.37e, 3.44e and 4.28e. If one assumes that the contributions from the top three orbital sets to the atomic population of Ni arise entirely from metal d orbitals with no contribution from the 4p orbitals to the t_2 populations, the above populations yield a d population of 9.09e, close to the closed sub-shell value of 10e. Subtracting the 9.09e and the 18e core from N(Ni) leaves ∼0.4e which represents the donation from ligands to the Ni. The t_2 orbital overlaps with both σ and π orbitals on CO, preventing one from obtaining a separate determination of the σ and π contributions to the ligands. Bauschlicher and Bagus [99] employ the CSOV method in their analysis of the bonding in both $Fe(CO)_5$ and $Ni(CO)_4$. They conclude that the Ni d shell is a filled d^{10} shell, that the CO σ donation is small, smaller than in the Fe complex, and that contributions from the metal 4s and 4p orbitals are very small. These

findings are in accord with the interpretation presented here.

8.4. $FeCp_2$

The HF electron configuration for the staggered D_{5d} geometry is $\ldots a_{1g}^2 a_{2u}^2 e_{2g}^4 e_{1u}^4 e_{1g}^4 : {}^1A_{1g}$. The two top levels are close in energy and their order is interchanged in the eclipsed D_{5h} geometry, an almost free rotation. The metal d orbitals transform as $e_{1g}(d_{xz}, d_{yz})$, $e_{2g}(d_{x2-y2}, d_{xy})$, $a_{1g}(d_{z2})$ and the contributions of these orbitals to the atomic population of iron N(Fe), are 0.52, 3.4 and 1.6e, respectively. Ascribing these contributions to the d orbitals gives a total d population of 5.5e compared to the free atom value of six. The populations of the e_{2g} and a_{1g} orbitals are largely localised on Fe, since they overlap with formally vacant antibonding combinations of the ring π systems.

Of the orbitals with a significant metal d contribution, the e_{1g} set interacts most strongly with the ligands with 0.5 of the four electrons contributing to N(Fe) and the remaining 3.5 populating the carbons of the Cp rings. Moffitt [58] argued that 'The primary source of the binding must therefore lie between the ligand e_{1g} and metal de_{1g} orbitals'. Frenking et al. state that when viewed as the interaction of a Fe^{+2} ion with two Cp^- rings, qualitative orbital arguments conclude that the electron donation from the occupied e_{1g} of $(Cp^-)_2$ should be the most important orbital contribution to the bonding. The p_x, p_y orbitals on Fe transform as e_{1u}, the set that describes the in phase (bonding) of the π orbitals on the two rings, a level that contributes 0.30e to N(Fe). The p_z orbital on Fe transforms as a_{2u} and overlaps with the out-of-phase overlap between the ring π systems. It contributes 0.08e to N(Fe). One cannot ascribe these populations solely to metal p orbitals, as density from the π systems of the Cp rings lie within the atomic domain of Fe. One can state that the molecular orbitals of the symmetry required to overlap with the metal p orbitals contribute only 0.4e to N(Fe).

9. The Laplacian of the density and donor–acceptor bonding

9.1. Laplacian of the density as the 3-D analogue of the conditional pair density

The Laplacian of a scalar function such as $\rho(r)$ has the property of locating where it is locally *concentrated*, where $\nabla^2\rho(r) < 0$, and locally *depleted*, where $\nabla^2\rho(r) > 0$. Since density is concentrated where $\nabla^2\rho(r) < 0$, one defines the function $L(r) = -\nabla^2\rho(r)$, such that a maximum in $L(r)$ denotes a maximum in the concentration of the density. One distinguishes between charge *concentrations* (CCs) and charge *depletions* (CDs) determined by the topology of $L(r)$, and charge *accumulations* and charge *reductions* determined by the differing topology of $\rho(r)$. $L(r)$ exhibits multiple valence maxima that are found to coincide with the number and relative positions of the localised electron pair domains that have been invoked in chemical models [102].

The topology exhibited by the Laplacian of the electron density in real space is a consequence of the electron pairing determined by the conditional pair density in six-dimensional space [65]. It is clear from Eq. (2) for the conditional pair density, that in a case wherein the Fermi hole of an electron of given spin is strongly localised about r_1, the conditional same-spin density will approach the single-particle spin density in regions r_2 removed from the region of localisation. In such regions, the conditional pair density approaches the total density ρ for a closed-shell system and consequently, its Laplacian distribution approaches the Laplacian of the electron density. Thus, the topologies of the two Laplacians exhibit a homeomorphism, one that approaches an isomorphic mapping of one field onto the other [65]. The local concentrations of the Laplacian of the conditional pair density indicate the positions where the remaining electron pairs will most likely be found relative to a reference pair and correspondingly, the CCs displayed in $L(r)$ signify the presence of *regions of partial pair condensation, that is, of regions with greater than average probabilities of occupation by a single pair of electrons*. This correspondence has been previously surmised because of the faithful mapping of the of the CCs of $L(r)$ with the number, relative size and angular orientation of the bonded and non-bonded electron pair domains assumed in VSEPR [103,104], a model originally rationalised on the investigations of the same-spin pair density by Lennard-Jones [61,64].It is important to understand that the concept of 'partial pair condensation' resulting from the homeomorphism, does not imply the association of a single pair of electrons with each CC, but rather, that the region of space so identified approaches unit pair population giving it a lower than average pair population. This reduction from the average pair population imbues the region with the properties associated with the bonded and non-bonded 'electron pairs' of chemistry, as made understandable in terms of the local expression for the virial theorem, Eq. (12)

$$\left(\frac{\hbar^2}{4m}\right)\nabla^2\rho(r) = 2G(r) + V(r) \tag{12}$$

$G(r)$ is the kinetic energy density and $V(r)$ the electronic potential energy density or virial field, whose sum equals H_b, the energy density at a bond CP. Since $G(r) > 0$ and $V(r) < 0$, a negative value for $\nabla^2\rho(r)$, as found at a CC in $L(r)$, indicates a region where $V(r)$ overrides the kinetic energy making the electronic potential energy density maximally stabilising, thus accounting for the role of bonded and non-bonded CCs as sites of nucleophilic activity or Lewis bases. The topology of the Laplacian of the density, both in its shell structure and in the number and arrangement of its local CCs plays a central role in the understanding of bonding in donor–acceptor complexes.

9.2. Atomic shell structure in L(r) and the question of 'missing' shells

It was noted early on that $L(r)$ exhibits shell structure by displaying alternating pairs of shells of charge concentration (the first one being a spike-like region centred on the nucleus) and charge depletion [105,106]. It is found that for atoms up to Xe, with the exception of transition metal atoms and including neighbouring metalloids, the structure determined in this manner duplicates that anticipated on the basis of equating the number of shells to the principal quantum number n [107,108]. For the transition metal atoms and metalloids (up to and including Ge in the fourth row) only $n-1$ such alternating pairs of shells are found. The 'missing' shell was interpreted by some [107] as a failure of the Laplacian, an interpretation dispelled by the demonstrated homeomorphism of $\nabla^2\rho(r)$ with that of the conditional pair density. Both Laplacians predict just three shells for Cr in the fourth row of the periodic table and four shells for Mo in the fifth row, for example. There is complete qualitative agreement between the two Laplacians regarding the number of shells, as well as excellent quantitative agreement in the values of the shell radii with only somewhat lesser agreement in the values of the associated extrema. The predicted number of shells is in agreement with the number observed in the experimentally determined radial distribution function [108].

Because of this demonstrated homeomorphism, one is forced to conclude that the outer and penultimate orbital shells of transition metal atoms are not physically distinct in terms of the localisation of the density within them. It is the outermost maximum in $L(r)$, the valence shell of charge concentration (VSCC), that determines the chemistry of an atom and the finding that the VSCC for heavy metal atoms is contiguous with the outer shell of the core is a reflection of the properties of the same-spin pair density for heavy metal atoms. Thus, the chemistry of these elements differs from that of their main group counterparts, differences previously attributed to the same cause by Gillespie et al. [109] Thus, unsurprisingly, one finds the distortions induced by bonding in the VSCCs of transition metal atoms differ from those found for their main group counterparts [110,111].

9.3. The atomic graph of a bound transition metal

Bonded interactions result in the formation of CCs on the surface of the outermost shell of charge concentration of an atom, a shell termed the valence shell charge concentration (VSCC). The CCs, (3, −3) CPs of $L(r)$, present in the VSCC of an atom define the vertices (V) of a polyhedron, the *atomic graph*, whose edges (E) are defined by the unique pairs of trajectories originating at intervening (3, −1) CPs and with each face (F) containing a (3, +1) CP. The atomic graph is denoted by the characteristic set [V, E, F] giving the number of each type of CP and the set satisfies Euler's relation that V − E + F = 2. It is the atomic graph that summarises the pairing of electrons in the valence shell of an atom and its vertices mimic the VSEPR model for non-transition metal atoms.

The VSEPR model can fail to predict the correct geometry when a transition metal or a pre-transition metal heavy metal atom such Ca, Sr or Ba, serves as the central atom for the assignment of the electron pair domains. Since the topology of $L(r)$ provides a model-free determination of the spatial localisation of the electrons that is present in any system, it can be used to determine the characteristics of the pair condensation for a bound transition metal atom and how they differ from those for a main group atom. This has been done for a wide selection of molecules containing transition and the preceding group II metal atoms [64,110,112,113]. These studies establish that it is indeed the outer shell of charge concentration of the core that is the VSCC of a transition metal. It is also found that, like main group molecules, the VSCC of the bonded metal atom exhibits a characteristic number of CCs and that the geometrical arrangement of these CCs appears to determine the most stable geometry of the molecule using a set of VSEPR-like rules. That is, the most stable geometry is the one that maximises the separations between the CCs or between the ligands and the CCs.

There is however, one striking difference in the behaviour of the CCs in the two cases that is most easily visualised in terms of the characteristic polyhedron generated by the CCs within the VSCC of the central atom. For a main group atom or a post-transition metal, the ligands are adjacent to some or all (depending on the number of non-bonded electron pairs) of the vertices of the polyhedron while in molecules containing a pre- or a transition metal atom, the ligands are adjacent to some or all of the faces of the same polyhedron. Thus, for main group and post-transition metal atoms, the ligands are linked to the local concentrations of electronic charge in its VSCC – the CCs act as bonded charge concentrations – while for pre-transition and transition metal atoms, the ligands are in general, linked to the critical points in the faces of the polyhedron, points that represent the sites of greatest charge depletion within the VSCC. In some cases, as are the equatorial ligands in $Fe(CO)_5$ discussed below, the ligands are linked to CPs defining the edges in the atomic graph. In an atomic graph whose vertices are opposite a face linked to a ligand, the metal atom exhibits *ligand opposed* CCs. Examples of this behaviour are found in the distorted tetrahedral geometry of CrO_2F_2 and in the square pyramidal geometries of VH_5 and $V(CH_3)_5$ [110]. Ligands may be linked to a CC in the VSCC of the metal when required by symmetry. This occurs for the axial ligands in the trigonal bipyramidal geometry in VF_5, the equatorial ligands being ligand opposed. Even in this case, the conditional pair density demonstrates that an axial CC of the metal is associated with its opposed ligand, so that even in such cases, the CCs are in fact, ligand opposed [64].

The ligand avoidance of the metal CCs is found for formally d^o transition metal complexes, for the pre-transition metals from Ca onwards in group II, and for the transition metal complexes with incomplete d shells, as exemplified

here by the carbonyl and Cp complexes. As described below, one may obtain the contribution of each molecular orbital to an atomic population. Such an analysis shows that $Ni(CO)_4$ has a d population of 9.0e, close to the closed-shell limit and its Laplacian distribution exhibits bonded rather than ligand opposed CCs. This holds true for the elements following it in the same row of the periodic table, the Ga atom in its dianion $[HGaGaH]^{-2}$exhibiting two bonded and one non-bonded CC. Other nickel complexes exhibit similar behaviour and Ni appears to mark the transition from one behaviour to the other.

9.4. Atomic graph representation of donor–acceptor interactions and crystal field splitting

The atomic graphs and three-dimensional representations of $L(r)$ for the metal atoms in the carbonyl complexes are shown in Fig. 7. The envelope diagram for Cr has been given previously [31]. The values of the CPs in $L(r)$ in the VSCC of the metal atom and their distances r from the nucleus are given in Table 9. The value of $L(r)$ at a (3, −3) CP and its distance r from the nucleus, are characteristic of the outer or valence shell charge concentration of the metal, the third quantum shell of M in each complex. The values of $L(r)$ increase and those for r decrease with increasing nuclear charge Z. The (3, −3) CPs have the smallest values of r, the distance increasing with the signature of the CP. The atomic graph for Cr is cubical, [8,12,6] and for Fe, a trigonal prism, [6,9,5].

Table 9
Laplacian critical points (atomic units)

Molecule	Type	$L(r)$	Distance r
$Cr(CO)_6$	(3, −3)	24.826	0.6778
	(3, −1)	19.797	0.6865
	(3, +1)	5.996	0.7162
	(3, +3)	−5.388	1.0320
$Fe(CO)_5$	(3, −3)	41.329	0.6096
	(3, −1)	38.452	0.6132
		25.140	0.6259
	(3, +1)	19.292	0.6351
		−8.066	0.9622
	(3, +3)	−10.225	0.9214
		−8.215	0.9697
$Ni(CO)_4$	(3, −3)	52.106	0.5619
	(3, −1)	51.211	0.5635
	(3, +1)	38.662	0.5732
	(3, +3)	−13.223	0.9019
$Fe(Cp)_2$	(3, −3)	46.518	0.6055
		74.261	0.5838
	(3, −1)	11.853	0.6456
	(3, +1)	11.845	0.6456
		−9.116	0.9431
	(3, +3)	−9.131	0.9431

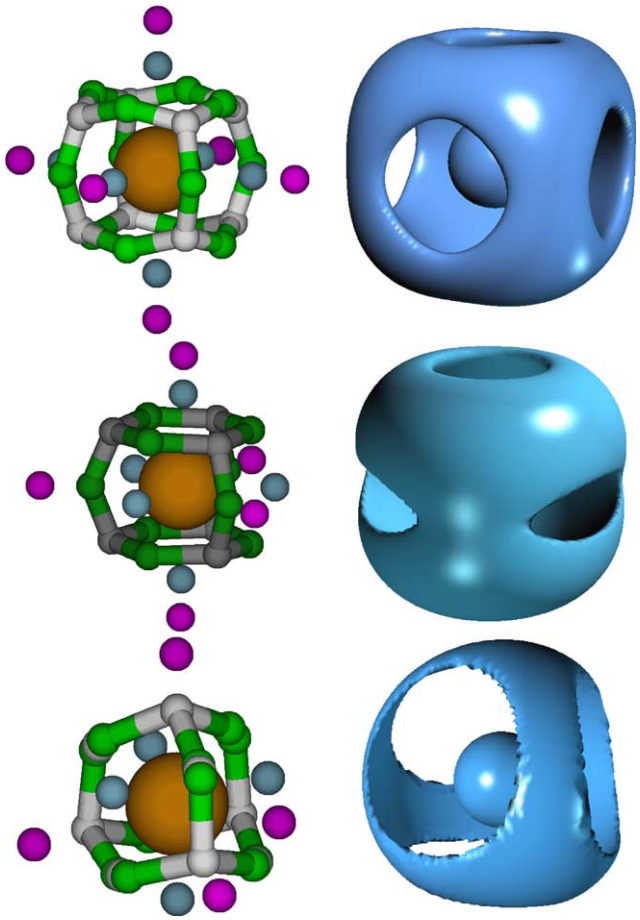

Fig. 7. Atomic graphs for the metal atoms in carbonyl complexes in the descending order Cr, Fe, and Ni. The trajectories linking the critical points in $L(r) = -\nabla^2\rho(r)$, are shown on the left and envelope plots on the right. The envelopes in the same order, have values of $L(r)$ = 22, 35 and 52 atomic units. The enclosed spheres indicate the inner cores. The colour scheme identifying the critical points in this and Fig. 9 is as follows; grey (3, −3); green (3, −1); blue (3, +1); purple (3, +3). The envelopes provide a striking visual display of the regions of charge concentration (CC) and charge depletion. In $Cr(CO)_6$ the CCs mimic the ligand avoiding t_{2g} set of crystal field orbitals and the ligands are adjacent to the octahedron of 'holes' that mimic the e_g set. In $Ni(CO)_4$ the ligands are adjacent to the tetrahedron of charge concentrations. One should bear in mind that the topology of the Laplacian is a property the total density and model-independent.

The atomic graph for Ni is derived from a regular tetrahedron with the characteristic set [4,6,4] by having each (3, −1) CP in an edge, bifurcate into a new (3, −3) vertex and two associated edge CPs, to yield the set [10,12,4]. However, the value of a sandwiched (3, −3) exceeds that the (3, −1) CPs by only 1×10^{-4} au and is the same distance from the nucleus. Consequently, the two sets of CPs are grouped together in Table 9. They are in close mutual proximity and this triplet of CPs is thus subject to coalescence resulting in its replacement by a single (3, −1) CP. Each triplet of CPs and its two associated vertices is topologically identical to the presence of a non-nuclear attractor in the electron density linking two nuclei. In the Cr complex, only CCs are susceptible to direct approach and thus the complex is susceptible to electrophilic

attack while the Ni complex, where both CDs and emergent CCs are free, should be susceptible to both nucleophilic and electrophilic attack. The Fe complex has free CCs for electrophilic attack and equatorial faces that, while bracketed by ligands, could serve as secondary centres for nucleophilic attack.

The diagrams in Fig. 8 display the CCs on the ligands, as well. One notes in particular, the large non-bonded CC on each carbon. These are directed at the holes, regions of charge depletion, in the atomic graph of Cr and at the axial holes in the atomic graph of Fe. The equatorial ligands in the Fe complex are directed at the CPs in the edges that separate the equatorial faces in the atomic graph. The CCs on the ligands in $Cr(CO)_6$ and on the axial ligands in $Fe(CO)_5$ give physical substance to the model of donor–acceptor interactions – the CC on the ligand being directed at a void on the metal atom [31]. In the nickel complex however, the non-bonded CCs on carbon are directed at the four equivalent tetrahedral vertices of the atomic graph for Ni. As noted previously, nickel has a d population of 9.0e, close to the closed-shell limit and its Laplacian distribution exhibits bonded rather than ligand opposed the CCs characteristic of the preceding transition metal atoms.

A (3, +3) CP, a 'hole' or local depletion in $L(r)$, lies on the line linking the non-bonded CC on a ligand carbon with a CP in the atomic graph of the metal. These (3, +3) CPs lie within the valence region of charge depletion and within the basin of the metal atom, being ∼0.8 au from the bond CP with the carbon, the bond CP itself lying from 1.7 to 1.8 au, Table 3. One such 'hole' is found opposite each of the faces of the octahedron in $Cr(CO)_6$ and opposite the two axial faces, as well as the (3, −1) CPs in the edges of the polyhedron in $Fe(CO)_5$. Four such holes are found in $Ni(CO)_4$ where, in this case, each links a vertex or CC of the atomic graph with a non-bonded CC on carbon. The presence of the (3, +3) CPs adjacent to the faces for an octahedral iron complex was noted previously by Bo et al. [114]. The linking of the CCs of the ligands with CPs on the metal with trajectories that emanate from an intervening (3, +3) CP is another difference between the bonding in a metal complex and that in main group molecules where the CCs on adjacent atoms are linked by a (3, −1) CP, just as two nuclear maxima are linked by a bond CP in the electron density.

In the crystal field description of an octahedral complex, the occupied t_{2g} set of orbitals that avoids the ligands lies lower in energy than the vacant e_g set that is directed at them. Bo et al. [114,115] note that the location of the maxima and minima in an atomic graph for a complex of O_h symmetry coincides with the pattern predicted by crystal field theory, with the CCs corresponding to the occupied t_{2g} set and the holes, or regions of charge depletion, CDs, corresponding to the empty e_g set. Macchi and Sironi [31] discuss the similarity exhibited by the density of the $(t_{2g})^6$ set of electrons in the Cr complex with the surface representation of the Laplacian distribution appearing in Fig. 7.

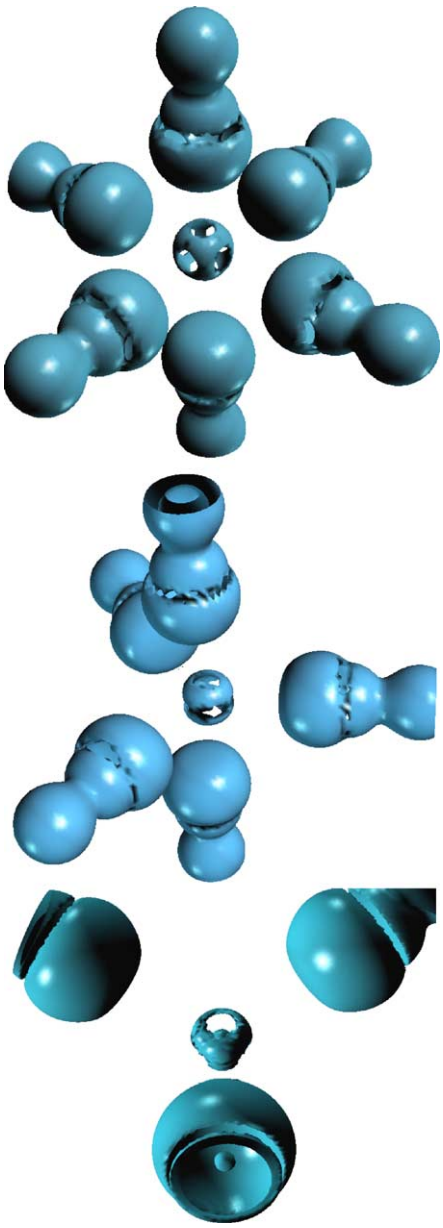

Fig. 8. Envelope maps of the metal atom within the ligand cage for the carbonyl complexes. The envelope for CO is for $L(r)$ = 0.0 au, the envelope enclosing the regions of charge concentration. Note the ring of charge depletion on each carbon adjacent to the non-bonded CC. The envelopes for the metal atoms are those used in Fig. 7. Of particular note are the pronounced non-bonded charge concentrations (CCs) on the carbons. They are directed at the 'holes' in the envelope for Cr in $Cr(CO)_6$, at the axial holes and ring of charge depletion on Fe in $Fe(CO)_5$ in the manner of a donor–acceptor complex. The charge concentrations on the Cr and Fe are directed at the regions of charge depletion associated with the ligand cage. In $Ni(CO)_4$, the non-bonded CCs on the carbons are directed at the charge concentrations on the Ni which behave as do bonded charge concentrations for main group atoms.

Ligand field theory distinguishes between the t_{2g} and e_g orbitals through their differing overlaps with the ligand orbitals, the former with π, the latter with sigma and it yields a modified interpretation of the atomic graph. The eight CCs in the Cr atomic graph are associated with the t_{2g} orbitals that

overlap with the π orbitals of the ligands, while the six faces or centres of charge depletion are associated with the e_g set that participate in σ bonding with the ligands. This association of the holes in the atomic graph with the σ bonding with Cr is in accord with the small transfer of charge from the ligand σ orbitals to Cr determined in the analysis of the orbital contributions to the atomic population on the Cr atom. The analysis shows that only 0.5 of the four electrons in the e_g set reside on the Cr atom, an observation further strengthening the donor acceptor interpretation of the Cr–C interaction.

The six CCs of the atomic graph for Fe are defined by the e″ set, and in ligand field theory, this set, like the t_{2g} of O_h, only overlaps with the ligand π orbitals and thus avoids the CCs on the ligands. Thus, the e″ orbitals coincide with the two rings of charge concentration in the atomic graph for iron and avoid the CCs on the ligands, Fig. 8. The dz^2 metal orbital of a_1' symmetry, overlaps only with the σ ligand orbitals and it is associated with regions of charge depletion in the atomic graph, the two axial holes. This association of the σ bonding of a_1' with holes in the VSCC of Fe is in accord with the small contribution of 0.33e of this orbital to the atomic population on Fe. The equatorial faces of the Fe atomic graph lie in the plane of the e′ set of orbitals that overlap with both σ and π orbitals on the ligands. The bonding behaviour of e′ is intermediate between that for the e″ and a_1' orbitals and this is reflected in its association with the three ligand CCs that are directed at neither CCs nor CDs in the atomic graph, but rather at the (3, −1) CPs defining the edges bounding the equatorial holes. A (3, −1) CP is a maximum in two-dimensions, as opposed to a three-dimensional maximum associated with a CC or vertex. Thus, the Fe atom retains 77% of the e″ set that avoids the CCs on the ligands and any σ bonding compared to 61% of the four electrons of the e′ orbitals that are engaged in both σ and π bonding in the equatorial plane and as opposed to the retention of only 17% of the two electrons in the a_1' orbital that donate to the σ orbitals on the ligands.

The nickel atom in $Ni(CO)_4$ is distinct in its bonding with the ligands in that the ligand CCs are directed at the CCs of the atomic graph of Ni, an apparent result of its possessing a nearly complete 3d shell. Both the lower energy t_2 orbital and the formally vacant (in crystal field theory) top t_2 orbital are occupied, the former contributing 1.4e to *N*(Ni), the latter, 4.3e. These orbitals overlap with both σ and π ligand orbitals and the four equivalent CCs at the vertices of the tetrahedron are directed at the ligand CCs in the manner of bonded CCs in the atomic graphs of main group atoms. The e set of orbitals, like the t_{2g} set in the Cr complex, can overlap only with π orbitals on the ligands but this set, which contributes 3.4e to *N*(Ni), defines the centres of charge depletion, the holes in the atomic graph for Ni, rather than the centres of charge concentration, as does the t_{2g} set in Cr.

The atomic graph for iron in $Fe(Cp)_2$, with the set [12,20,10], like chromium hexacarbonyl, provides a striking example of ligand avoidance by the CCs of a transition metal. The atomic graph and its relation to the Laplacian distribution of the Cp rings are displayed in Fig. 9. The CCs of the

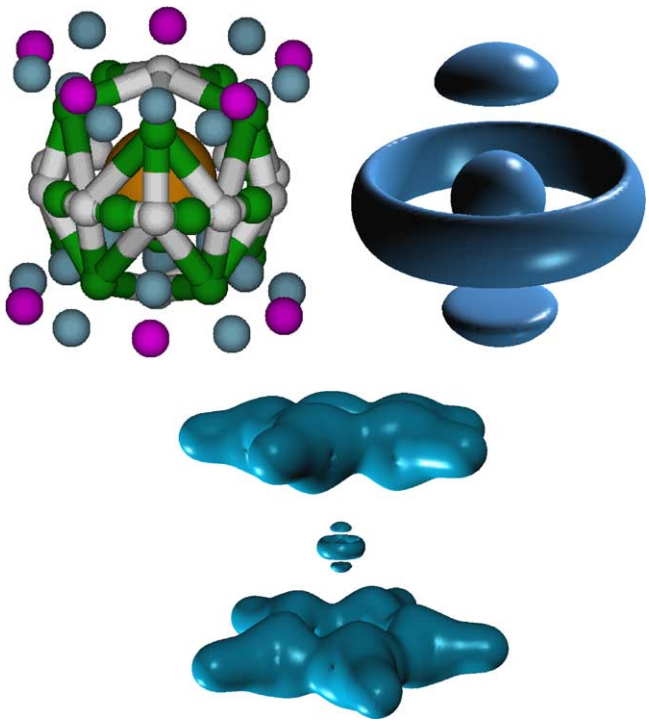

Fig. 9. Atomic graph for the iron atom in ferrocene and its envelope for $L(r)$ = 45 atomic units. Also shown is an envelope for the entire complex, using the zero envelope for the ligands in the representation of $L(r)$ for the entire complex. The two axial CCs and the equatorial belt of charge concentration on Fe mimic the ligand field a_{1g} and e_{2g} orbitals that avoid σ bonding with the ligands, being instead directed at the regions of charge depletion in the centre of each Cp ring and at the intervening region between them. The secondary charge concentration of the π system in each of the Cp rings is directed at the equatorial rings of charge depletion on Fe.

atomic graph, like the e_{2g} and a_{1g} orbitals, avoid the charge concentrations on the ligands. The e_{2g} orbitals correlate with the equatorial belt of charge concentration and the a_{1g} with the two axially opposed CCs, the latter two dominating the atomic graph. They are directed at (3, +1) CPs or centre of charge depletion found in the face of each Cp ring, with $L(r)$ = −0.27 au. Eighty-five and 80% of the e_{2g} and a_{1g} populations, respectively, reside on the Fe atom, since they overlap only with π orbitals on the ligands. The axial CCs on Fe are of larger magnitude than the ring of 10 CCs that form a belt of charge concentration parallel with and lying between the two Cp rings. The 10 CCs in the belt alternate with 10 (3, −1) CPs that are of equal value to within one-thousandth of an au and the belt thus signifies the presence of a ring of essentially constant concentration of electronic charge inter-spaced between the two Cp rings. There are in addition, two rings of five (3, −1) CPs, each ring linking one of the axial maxima with the maxima in the belt of charge concentration.

The delocalized π density in an aromatic system results in the presence of two (3, −1) CPs in the atomic graph of a carbon, one on each side of the ring [116]. These CPs are two-dimensional maxima with $L(r)$ = 0.15 au, maxima that are evident on each side of the Cp rings in the envelope plot of their Laplacian distributions, Fig. 9. These secondary maxima

on the carbons are directed at the two circular rings of charge depletion defined by the two sets of five (3, +1) CPs in the atomic graph for iron. The rings of charge depletion correlate with the e_{1g} orbitals which interact strongly with the ligands and retain only 13% of their four electrons on Fe.

As in the carbonyl complexes, a (3, +3) CP lies on the line linking a two-dimensional maximum on a ring carbon with a (3, +1) CP in the atomic graph for iron. Thus, the rings of charge depletion are linked to the CCs of the carbons of the rings via rings of (3, +3) CPs, the local 'holes' in each ring being interspaced with (3, +1) CPs of slightly smaller magnitude.

The observation that the non-bonded CCs on the carbons are directed at regions of charge depletion on the metal in the Laplacian distributions for $Cr(CO)_6$, $Fe(CO)_5$ and $FeCp_2$, as depicted in Fig. 8 and Fig. 10, provide a pictorial representation of the donor–acceptor bonding ascribed to the metal complexes with the ligands as donors and the metals as the acceptor. But what the Laplacian distributions also illustrate is that the CCs on the metal are in turn directed at regions of charge depletion between or on the ligands as well, a prime example being the two axial CCs on Fe in ferrocene being directed at the regions of charge depletion in the interior of each Cp ring. Missing from the usual interpretation of such interactions is the realisation that both participants assume dual roles as both donors and acceptors. This view is clearly brought to the fore by the presence of CCs on the metal atom and their role as donors with respect to the ligands, the presence of which are not made clear in the orbital models of such interactions. The donor action of the metal CCs in $Cr(CO)_6$ is a reflection of the D–C–D back bonding model. There is no physical distinction between the CCs of the ligands being directed at voids on the metal and the CCs of the metal being directed at voids on the ligands, the overall effect calling to mind Ehrlich's 'lock and key' analogy of an enzyme-substrate interaction and his introduction of the concept of a 'receptor' into physiological chemistry [117].

10. Summary and conclusions

All bonding is a result of the stabilising decrease in the electrostatic interaction of the nuclei with the electron density, the term ΔV_{en}, and in particular, from the interaction of the density of each reactant with the nuclei of the other reactants assembled in the product molecule, the external contribution ΔV_{en}^{e}. These contributions are of greater magnitude for homopolar (covalent) molecules N_2 and C_2 than for their isoelectronic congeners the polar CO and the ionic LiF and there is no physical basis for ascribing a 'covalent contribution' as opposed to the 'electrostatic force' as the source of bonding.

The bonding in the metal donor–acceptor complexes is understandable in terms of quantities defined by quantum mechanics obviating the need to partition the process into a series of physically unrealisable steps. The energy of formation of a metal carbonyl complex is a result of the dominant and exceptional decrease in the electrostatic energy of interaction of the electron density of the metal atom with the nuclei of the surrounding cage of ligand nuclei, the term $\Delta V_{en}^{e}(M)$ and from the stabilisation of the carbon atoms resulting from the transfer of density to carbon from the metal atom, the transferred density causing both the internal and external contributions to $\Delta V_{en}(C)$ to contribute to the stabilisation. The major interatomic charge transfer is from the metal to the carbons of the ligands accompanied by a much smaller transfer from the oxygens. The charge transfer from M to each C, in the amount of 0.1–0.2e, is relatively small in accord with the bonding density being nearly equally shared by both atoms. The delocalization indices δ(M, C) are of the order unity, quantifying the notion that the M–C 'resonance stabilisation' or 'covalency' results from the exchange of approximately one $\alpha\beta$ pair. The extent of exchange of the density on the metal atom with the surrounding cage of carbons is dramatically evidenced in the substantial increase in the degree of delocalisation of the density of a carbon atom on complexation. The major transfer of charge from the metal to the carbons is via the D–C–D $d\pi$–$p\pi^*$ back donation mechanism one that, judged by the change in the carbon atomic quadrupole moment, is a maximum for the equatorial carbon in the iron complex and decreases in the order Fe(eq C) > Ni > Cr > Fe (ax C).

The sole interatomic charge transfer in the formation of ferrocene is from the metal to the carbon atoms, in the amount of 0.4e per ring. There is a sharing of two Lewis pairs between Fe and the carbon atoms of each ring, the exchange density being delocalized over the surface of the bonded cone of density defined by the bond paths linking the Fe atom to each ring. It is the attraction of the density of the metal atom M with all the nuclei *external* to the basin of M, the contribution $V_{en}^{e}(M)$, that dominates the stabilisation of ferrocene and germanocene, and the bonding is a result of the net stabilisation of the density on M in its interaction with the atoms of the ligands.

Frenking et al. [25] state that the bonds in ferrocene are equally the result of 'electrostatic forces' and 'covalent bonding' using EDA. In addition to this partitioning of the energy being arbitrary, the mechanism or force operative in 'covalent bonding', as opposed to that from the 'electrostatic force', is never explained, its contribution being ascribed to the relaxation of the orbitals to their final form. The same potential energy operators, the electron–nuclear V_{en} and the electron–electron V_{ee} interactions, are averaged over the wave function in every step of the EDA and are the sole cause of the changes in potential energy, regardless of the name one ascribes to it. Since the states involved in the steps are not quantum states, one cannot use the virial theorem to relate changes in the energy to changes in the potential energy. Indeed, one cannot be certain that the final energy decrease ascribed to 'orbital relaxation/covalent bonding' is not due to a decrease in the repulsive contributions from V_{ee} rather than to a stabilizing decrease in V_{en}. In brief, one has no phys-

ical understanding of what forces or interactions constitute 'covalent bonding' and the mystery surrounding this term is understandable.

References

[1] R.F.W. Bader, Atoms in Molecules: A Quantum Theory, Oxford University Press, Oxford UK, 1990.
[2] F.A. Cotton, A.H. Cowley, X. Feng, J. Am. Chem. Soc. 120 (1998) 1795.
[3] Y. Xie, R.S. Grev, J. Gu, H.F. Schaefer, P. Schleyer, J. Su, X.-W. Li, G.H. Robinson, J. Am. Chem. Soc. 120 (1998) 3773.
[4] T.L. Allen, W.H. Fink, P.P.J. Power, J. Chem. Soc., Dalton Trans. (2000) 407.
[5] J.M. Molina, J.A. Dobado, G.L. Heard, R.F.W. Bader, M.R. Sundberg, Theor. Chem. Acc. 105 (2001) 365.
[6] S. Srebrenik, R.F.W. Bader, J. Chem. Phys. 63 (1975) 3945.
[7] R.F.W. Bader, S. Srebrenik, T.T. Nguyen Dang, J. Chem. Phys. 68 (1978) 3680.
[8] R.F.W. Bader, Phys. Rev. B 49 (1994) 13348.
[9] P.A.M. Dirac, The Principles of Quantum Mechanics, Oxford University Press, Oxford, 1958.
[10] There is considerable confusion regarding the use of the words 'observable' and 'measurable' in the literature. This paper follows the definitions and use given by Dirac [9], page 37: "We call a real dynamical variable (a linear Hermitian operator) whose eigenstates form a complete set an *observable*." Dirac continues "Thus, any quantity that can be measured is an observable. The question presents itself—can every observable be measured? . . ." Expectation values may or may not be measurable, the expectation value of the Hamiltonian operator, the energy, being an example of a property for which only differences can be obtained from experiment.
[11] J.C. Slater, Quantum Theory of Molecules and Solids. I, McGraw-Hill Book Co. Inc., New York, 1963.
[12] J. Schwinger, Phys. Rev. 82 (1951) 914.
[13] S. Srebrenik, R.F.W. Bader, T.T. Nguyen-Dang, J. Chem. Phys. 68 (1978) 3667.
[14] R.F.W. Bader, Theor. Chem. Acc. 105 (2001) 276.
[15] R.F.W. Bader, Theor. Chem. Acc. 107 (2002) 381.
[16] C.C.J. Roothaan, Rev. Mod. Phys. 23 (1951) 69.
[17] R.S. Mulliken, Phys. Rev. 32 (1928) 186.
[18] R.S. Mulliken, Rev. Mod. Phys. 2 (1930) 60.
[19] R.S. Mulliken, Rev. Mod. Phys. 3 (1931) 89.
[20] F. Hund, Z. Phys. 51 (1928) 759.
[21] G. Herzberg, Molecular Spectra and Molecular Structure. D, Van Nostrand Co. Inc., New York, 1950.
[22] R.F.W. Bader, Can. J. Chem. 40 (1962) 1164.
[23] E. Schrödinger, Ann. D. Phys. 81 (1926) 109.
[24] G. Frenking, N. Frölich, Chem. Rev. 100 (2000) 717.
[25] G. Frenking, K. Wichmann, N. Frölich, C. Loschen, M. Lein, J. Frunzke, V.M. Rayón, Coord. Chem. Rev. 238/239 (2003) 55.
[26] G. Frenking, Angew. Chem. Int. Ed. Engl. 42 (2003) 143.
[27] R.J. Gillespie, P.L.A. Popelier, From Lewis to Electron Densities, Oxford University Press, 2001.
[28] R.F.W. Bader, Int. J. Quantum Chem. 94 (2003) 173.
[29] K. Morokuma, J. Chem. Phys. 55 (1971) 1236.
[30] T. Ziegler, A. Rauk, Theor. Chem. Acta 46 (1977) 1.
[31] P. Macchi, A. Sironi, Coord. Chem. Rev. 238-239 (2003) 383.
[32] W. Kohn, L.J. Sham, Phys. Rev. A 140 (1965) 1133.
[33] K.L. Kunze, E.R. Davidson, J. Phys. Chem. 96 (1992) 2129.
[34] T. Ziegler, V. Tschinke, C. Ursenbach, J. Am. Chem. Soc. 109 (1987) 4825.
[35] B.J. Persson, P.R. Taylor, Theor. Chem. Acc. 110 (2003) 211.
[36] J.C. Greene, Chem. Soc. Rev. 27 (1998) 263.
[37] F. Benabicha, V. Pichon-Pesme, C. Jelsch, C. Lecomte, A. Khmou, Acta Crystallogr. B56 (2000) 155.
[38] R. Flaig, T. Koritsanszky, B. Dittrich, A. Wagner, P. Luger, J. Am. Chem. Soc. 124 (2002) 3407.
[39] R. Kingsforf-Adaboh, B. Dittrich, A. Wagner, M. Messerschmidt, R. Flaig, P. Luger, Z. Kristallogr. 217 (2002) 168.
[40] R. Flaig, T. Koritsánszky, D. Zobel, P. Luger, J. Am. Chem. Soc. 120 (1998) 2227.
[41] B.K.T. Dittrich, M. Grosche, W. Scherer, R. Flaig, A. Wagner, H.G. Krane, H. Kessler, C. Riemer, A.M.M. Schreurs, P. Luger, Acta Crystallogr. B58 (2002) 721.
[42] C.F. Matta, R.F.W. Bader, Proteins: Struct. Funct. Genet. 52 (2003) 360.
[43] F.J. Martìn, PhD Thesis, McMaster University, 2001.
[44] R.F.W. Bader, P.L.A. Popelier, T.A. Keith, Angew. Chem. Int. Ed. Engl. 106 (1994) 647.
[45] R.F.W. Bader, D. Bayles, J. Phys. Chem. A 104 (2000) 5579.
[46] F. Cortes, R.F.W. Bader, Chem. Phys. Lett. 379 (2003) 183.
[47] P.V. Schleyer, (Ed.), Encyclopedia of Computational Chemistry, vol. 1, John Wiley and Sons, Chichester, UK, 1998, p. 64.
[48] It is irrelevant that some group contributions predicted by QTAIM were measured previously, those by Pascal in 1910 and by Rossini and co-workers in 1945. Recovery of established observations as a test of theory is as old as Newton and exemplified in QM: (1) by Schrödinger's first paper in his recovery of the quantization of angular momentum and energy and the prediction of the Lyman and Balmer spectra of the hydrogen atom, and (2) by Schwinger's calculation of the anomalous magnetic moment of the electron following its measurement by Rabi and co-workers, an important step in the development of QED. The demonstration that measured values of group properties are predicted by QM, while perhaps less momentous, is of vital importance to an experimental chemist.
[49] R.F.W. Bader, J. Phys. Chem. A 102 (1998) 7314.
[50] All interacting atoms, atoms that share a common interatomic surface, are linked by an atomic interaction line, whether the interaction be attractive or repulsive. For interatomic separations corresponding to motion within a bound potential well, the forces on the nuclei are such as to return the system to its equilibrium geometry where the forces vanish and the atomic interaction line is designated a bond path. The approach of two Ar atoms is initially attractive to yield a van der Waals minimum of 0.012 ev at a separation of 7.1 au and the atoms are linked by a bond path. For energies in excess of the well depth, the forces on the nuclei will be repulsive, the atoms will be linked by an atomic interaction line and the molecule will dissociate.
[51] R.F.W. Bader, Y. Tal, S.G. Anderson, T.T. Nguyen-Dang, Isr. J. Chem. 19 (1980) 2871.
[52] T.S. Koritsanszky, P. Coppens, Chem. Rev. 101 (2001) 1583.
[53] R.F.W. Bader, T.T. Nguyen-Dang, Y. Tal, Rep. Prog. Phys. 44 (1981) 893.
[54] T.A. Keith, R.F.W. Bader, Y. Aray, Int. J. Quantum Chem. 57 (1996) 183.
[55] A structural homeomorphism exists between the densities of the electrons and virial field. For a system close to a singularity, it is possible for the geometries at which the two fields cross a structural boundary to differ. The systems under study in the present paper are far removed from any singularities.
[56] C.F. Matta, T.T.H.J. Hernández-Trujillo, R.F.W. Bader, Chem. Eur. J. 9 (2003) 1940.
[57] R.F.W. Bader, C.F. Matta, F. Cortes-Guzman, Organometallics, accepted for publication.
[58] W. Moffitt, J. Am. Chem. Soc. 76 (1954) 3386.
[59] J. Lennard-Jones, Adv. Sci. Lond. 11 (1954) 136.
[60] J. Lennard-Jones, J. Chem. Phys. 20 (1952) 1024.
[61] J.E. Lennard-Jones, Proc. R. Soc. Lond. Ser. A 198 (1949) 14.
[62] R.J. Gillespie, R.S. Nyholm, Q. Rev. Chem. Soc. 11 (1957) 239.
[63] R.J. Gillespie, Prog. Stereochem. 2 (1958) 261.

[64] R.J. Gillespie, D. Bayles, J. Platts, G.L. Heard, R.F.W. Bader, J. Phys. Chem. A 102 (1998) 3407.
[65] R.F.W. Bader, G.L. Heard, J. Chem. Phys. 111 (1999) 8789.
[66] R.F.W. Bader, M.E. Stephens, J. Am. Chem. Soc. 97 (1975) 7391.
[67] X. Fradera, M.A. Austen, R.F.W. Bader, J. Phys. Chem. A 103, 304.
[68] R. Daudel, M.E. Stephens, E. Kapuy, C. Kozmutza, Chem. Phys. Lett. 40 (1976) 194.
[69] (a) J. Poater, M. Solà, M. Duran, X. Fradera, Theor. Chem. Acc. 107 (2002) 362;
(b) T. Kar, J.C. Ángyán, A.B. Sannigrahi, J. Phys. Chem. A 104 (2000) 9953.
[70] M.A. Austen, PhD Thesis, McMaster University, 2003.
[71] D. Cremer, E. Kraka, Angew. Chem. 23 (1984) 627.
[72] P. Macchi, D.M. Proserpio, A. Sironi, J. Am. Chem. Soc. 120 (1998) 13429.
[73] R.F.W. Bader, C.F. Matta, Inorg. Chem. 40 (2001) 5603.
[74] R.F.W. Bader, D.A. Legare, Can. J. Chem. 70 (1992) 657.
[75] R.F.W. Bader, H.J.T. Preston, Int. J. Quantum Chem. 3 (1969) 327.
[76] R.F.W. Bader, in: T.B.M. Deb (Ed.), The Force Concept in Chemistry, Van Nostrand Reinhold Co., New York, 1981, p. 39.
[77] K. Morokuma, Acc. Chem. Res. 10 (1977) 294.
[78] J.C. Slater, J. Chem. Phys. 57 (1972) 2389.
[79] R.F.W. Bader, C.F. Matta, J. Phys. Chem. A, in press (2004).
[80] J. Hernández-Trujillo, R.F.W. Bader, J. Phys. Chem. A 104 (2000) 1779.
[81] M.T. Carroll, R.F.W. Bader, Mol. Phys. 65 (1988) 695.
[82] T. Berlin, J. Chem. Phys. 19 (1951) 208.
[83] R.F.W. Bader, W. Henneker, J. Am. Chem. Soc. 87 (1965) 3063.
[84] R.F.W. Bader, W.H. Henneker, P.E. Cade, J. Chem. Phys. 46 (1967) 3341.
[85] R.P. Feynman, Phys. Rev. 56 (1939) 340.
[86] G. Das, A.C. Wahl, J. Chem. Phys. 44 (1966) 87.
[87] J.C. Slater, Phys. Rev. 81 (1951) 385.
[88] J.C. Slater, C Notes: 8–15, in: Quantum Theory of Atomic Structure, McGraw-Hill, New York, 1960.
[89] A.M. Pendás, E. Francisco, M.A. Blanco, J. Chem. Phys. 120, 4581.
[90] R.F.W. Bader, H.J.T. Preston, Can. J. Chem. 44 (1966) 1131.
[91] L. Salem, Proc. R. Soc. Lond. Ser. A 264 (1961) 379.
[92] R.F.W. Bader, J.R. Cheeseman, K.E. Laidig, C. Breneman, K.B. Wiberg, J. Am. Chem. Soc. 112 (1990) 6530.
[93] F. Cortes-Guzman, J. Hernandez-Trujillo, G. Cuevas, J. Phys. Chem. A 107 (2003) 9253.
[94] A.E. Reed, L.A. Curtiss, F. Weinhold, Chem. Rev. 88 (1988) 899.
[95] S. Dapprich, G. Frenking, J. Phys. Chem. 99 (1995) 9352.
[96] R.F.W. Bader, P.F. Zou, Chem. Phys. Lett. 191 (1992) 54.
[97] M. Dewar, Bull. Soc. Chim. Fr. (1951) C79.
[98] J. Chatt, L.A. Duncanson, J. Chem. Soc. (1953) 2329.
[99] C.W. Bauschlicher, P.S. Bagus, J. Chem. Phys. 81 (1984) 5889.
[100] G.L. Miessler, D.A. Tarr, Inorganic Chemistry, second ed., Prentice Hall, New Jersey, 1998.
[101] I.H. Hillier, V.R. Saunders, Mol. Phys. 22 (1971) 1025.
[102] R.F.W. Bader, P.J. MacDougall, C.D.H. Lau, J. Am. Chem. Soc. 106 (1984) 1594.
[103] R.J. Gillespie, Molecular Geometry, Van Nostrand Reinhold, London, 1972.
[104] R.J. Gillespie, I. Hargittai, The VSEPR Model of Molecular Geometry, Allyn and Bacon, Boston, MA, 1991.
[105] R.F.W. Bader, P.M. Beddall, J. Chem. Phys. 56 (1972) 3320.
[106] R.F.W. Bader, H. Essén, J. Chem. Phys. 80 (1984) 1943.
[107] R.P. Sagar, A.C.T. Ku, V.H. Smith, J. Chem. Phys. 88 (1988) 4367.
[108] Z. Shi, R.J. Boyd, J. Chem. Phys. 88 (1988) 4375.
[109] R.J. Gillespie, D.A. Humphreys, N.C. Baird, E.A. Robinson, Chemistry, Allyn and Bacon, Boston, 1986.
[110] R.J. Gillespie, I. Bytheway, T.-H. Tang, R.F.W. Bader, Inorg. Chem. 35 (1996) 3954.
[111] R.F.W. Bader, Coord. Chem. Rev. 197 (2000) 71.
[112] R.F.W. Bader, S. Johnson, T.-H. Tang, P.L.A. Popelier, J. Phys. Chem. A 100 (2000) 15398.
[113] I. Bytheway, R.J. Gillespie, T.-H. Tang, R.F.W. Bader, Inorg. Chem. 34 (1995) 2407.
[114] C. Bo, J.-P. Sarasa, J.-M. Poblet, J. Phys. Chem. 97 (1993) 6362.
[115] C. Bo, J.M. Poblet, M. Bénard, Chem. Phys. Lett. 169, 89.
[116] R.F.W. Bader, C. Chang, J. Phys. Chem. 93 (1989) 2946.
[117] P. Ehrlich, Lancet 2 (1913) 445.